



FACULTY OF SCIENCE AND TECHNOLOGY

MASTER'S THESIS

Study programme/specialisation:
Marine and Offshore Technology

Spring/ Autumn semester, 2020

Open / Confidential

Author: Rinat Khaziev

A handwritten signature in black ink, appearing to be 'RKhaziev'.

Programme coordinator: Muk Chen Ong

Supervisor(s): Ove Tobias Gudmestad (UiS),
Anatoly Borisovich Zolotukhin (Gubkin University)

Title of master's thesis:
APPLICATION OF NEW TECHNOLOGICAL SOLUTIONS FOR IMPROVING
DEVELOPMENT EFFICIENCY OF THE KORCHAGIN FIELD

Credits: 30 ECTS

Keywords: Caspian Sea, Offshore
Development, Korchagin Field, Gas
Breakthrough, Hydrodynamic Model, Ice
Model Tests, Barrier Well.

Number of pages: 89
+ supplemental material/other:

Stavanger, June 15, 2020

Abstract

In this thesis oil and gas condensate Yu. Korchagin field is considered. It is located in the northern part of the Caspian Sea. Thus, production at this field is complicated by both marine production conditions and Arctic conditions in the winter season. One of the main difficulties associated with field development is the presence of a massive overlying gas cap and underlying water, where the oil rim has a thickness of only 20 m.

In the master's thesis, an analysis of the reasons for the gas factor growth during the operation of horizontal wells was made, as well as its influence on the development parameters of the Yu. Korchagin field. The theoretical part of the work covers a description of the climatic, geological and geographical conditions of the field, as well as a description of the technical and technological components of the field development project.

In the calculation part, a description of the design solution to limit gas and water inflow to the well is presented, which consists in the use of additional production wells in the gas- and water-saturated parts. Also, the technological and economic efficiency of the proposed solution was evaluated. The calculations were carried out using a hydrodynamic simulator.

Acknowledgements

I would like to express my gratitude to the Gubkin Russian State University of Oil and Gas (National Research University) and the University of Stavanger for giving me an opportunity to study, to gain new experience and to do this Master Thesis.

I am very grateful to the supervisors of my work Professor Anatoly Zolotukhin and Professor Ove Tobias Gudmestad for their work, continuous support and advice. Without their guidance, useful comments, immense field knowledge, engagement, and patience, this master thesis would not have been possible.

I also want to thank my family, who supported my choice to enter this joint master's program and helped me throughout the studying.

List of contents

List of abbreviations	6
List of figures.....	7
List of tables	9
Introduction	10
Chapter 1. Yu. Korchagin Field Description.....	11
1.1. Geography and Physical Environment	11
1.2. Geological Description	14
1.3. Physico-chemical Properties of Formation Fluids.....	17
1.4. Field development experience	18
1.5. Complicating Field Development Factors	21
Chapter 2. The technical part	22
2.1. Technical facilities at the Yu. Korchagin field.....	22
2.2. Ice model tests of IRP-1	26
2.3. IRP-1 and single buoy mooring construction	31
2.4. Floating oil storage	35
2.5. Satellite platform	36
Chapter 3. The technological part	39
3.1. Description of the current state of field development	39
3.2. Field development control	43
3.3. Field pilot works.....	46
3.4. Analysis of the project document decisions implementation at the initial stage of development	51
3.5. Reasons of gas breakthrough and ways to minimize them.....	54

3.6.	Recommendations for field development regulation.....	57
Chapter 4.	Calculation part.....	60
4.1.	Analysis of the existing field development concept	60
4.2.	Analysis of the gas-oil ratio influence on the reserve recovery	60
4.3.	Hydrodynamic model	67
4.4.	Restriction of gas and water inflow to a horizontal oil producing well	74
4.5.	Feasibility study.....	80
4.6.	Technological risks analysis and ways to minimize them.....	82
Conclusion	85
References	86

List of abbreviations

ASPA	–	Astrakhan Shipbuilding Production Association
FSI	–	FloScanImager
GOC	–	Gas-Oil Contact
GOR	–	Gas-Oil Ratio
HCG	–	Hydrocarbon Gases
IPE RAS	–	Institute of Physics of the Earth of the Russian Academy of Sciences
IRP	–	Ice Resistant Platform
OWC	–	Oil-Water Contact
TAML	–	Technology Advancement for Multi-Laterals
TCS	–	Temperature Control System

List of figures

Fig. 1.1.1. Overview of the Russian sector in the Northern Caspian [1]	11
Fig. 1.1.2. Dynamics of the water level of the Caspian Sea [5]	13
Fig. 1.1.3. Average surface temperature of the Caspian Sea [8]	14
Fig. 1.2.1. Geological profile of the Neocomian stage [9]	15
Fig. 1.2.2. Comparison of the initial and current sections of the lithology of the geological and technological model [10]	16
Fig. 1.4.1. Main technological parameters for the development of Yuri Korchagin field [10]	19
Fig. 1.4.2. The lengths of horizontal wells drilled in the Yu. Korchagin field throughout the period of the development [10]	20
Fig. 2.1 Complex of offshore facilities of the Yu. Korchagin field [13]	23
Fig. 2.2 Schematic representation of the oil treatment installation [15]	25
Fig. 2.3 General view of IRP-1 model [13]	27
Fig. 2.4 Experimental setup for direct motion test [13]	28
Fig. 2.5 Forming ice rubble accumulations in front of IRP-1 model [13]	29
Fig. 2.6 Comparison of time histories obtained in both direct- and reversed-motion modes [13]	30
Fig. 2.7 Horizontal ice-force time history and peak best-fit line in case of formation of grounded rubble. [13]	31
Fig. 2.8 Floating crane «Bogatyr-3» [17]	33
Fig. 2.9 Floating crane «Volgar» [18]	33
Fig. 2.10 Single buoy mooring [20]	35
Fig. 2.11 Offshore transshipping complex [20]	36
Fig. 2.12 Upper part of the satellite platform [22]	37
Fig. 3.1 Schematic diagram of the flow regulation system layout in well 11 [22]	48
Fig. 3.2 Adaptive inflow control device option [22]	49
Fig. 3.3 The schematic diagram of the intellectual completion of well 13 [22]	51

Fig. 3.4 Oil-gas ratio values on the area of the field [22]	55
Fig. 3.5 The dependence of the increase in the oil-gas ratio from the angle of productive deposits incidence and the time of the well operation [22]	56
Fig. 4.1 Well №1 performance dynamics	61
Fig. 4.2 Cross section of horizontal well development element [33]	62
Fig 4.3 Critical flow rate dynamics	66
Fig. 4.4 Distribution of a) permeability in the XY direction; b) permeability in the Z direction; c) porosity	68
Fig. 4.5 PVT characteristics of oil. Dependence on pressure of: a) gas content, b) volume factor, c) density, d) viscosity	69
Fig. 4.6 PVT characteristic of gas. Dependence on pressure of: a) density, b) viscosity	70
Fig. 4.7 Dependences of relative phase permeabilities for the system a) oil-water, b) oil-gas	71
Fig. 4.8 Dependences of capillary pressure for the oil-water and oil-gas systems	72
Fig. 4.9 Distribution of a) gas saturation, b) oil saturation, c) water saturation	73
Fig 4.10 Initial reservoir pressure distribution	73
Fig. 4.11 3-D model view for the single well case	75
Fig. 4.12 Dynamics of oil, gas flowrates and water cut for the single well case	75
Fig. 4.13 3-D model view for the two wells case	76
Fig. 4.14 Dynamics of oil, gas flowrates and water cut for the two wells case	77
Fig. 4.15 3-D model view for the three wells case	78
Fig. 4.16 Dynamics of oil, gas flowrates and water cut for the three wells case	78
Fig. 4.17 Dynamics of cumulative oil production for three cases	79

List of tables

Table 2.1	Test modes selected for analysis [13]	28
Table 3.1	Implementation status of the project wells for January 1, 2020 [24]	40
Table 3.2	Well number characteristics for 01.01.2020 [24]	41
Table 4.1	The initial data for the Q_{cr} calculation [35]	63
Table 4.2	The calculated values of Q_{cr} for well No. 1	64
Table 4.3	Initial data for PVT model	70
Table 4.4	Parameters for model initialization	73
Table 4.5	Oil producing well parameters	74
Table 4.6	Comparison of cumulative oil production with a base case	79
Table 4.7	Well construction investment costs [35]	81
Table 4.8	Product sales revenue	81
Table 4.9	Revenue from product sales for the entire field	82
Table 4.10	Key recommendations for risks minimizing	84

Introduction

Russia is one of the main participants in the global market for the production, transport and realizing of hydrocarbons and is focused on maintaining their production levels. As the largest oil and gas provinces (Volga-Ural, West Siberian, etc.) are depleted, exploration work is shifting to more inaccessible regions (Arctic and marine).

Yuri Korchagin field is located on the Russian shelf of the northern part of the Caspian Sea. Thus, production at this field is complicated by both marine production conditions and Arctic conditions in the winter season. This field is the first field in Russia to be developed under such conditions, and the development is undoubtedly of great interest from the point of view of research and practical activities.

The aim of this work is to identify the main difficulties associated with the efficient development of reserves, as well as the introduction of new fundamental approaches for the development of the reservoirs with a massive gas cap and an active aquifer.

The objectives of this work are to study the existing conditions for the development of the field, analyze the reasons for the gas-oil ratio growth during the production phase, as well as assess the effectiveness of the use of barrier wells for gas and water breakthrough limitation. For this purpose, a hydrodynamic model was built and calculated for three cases with different number of wells.

Chapter 1. Yu. Korchagin Field Description

1.1. Geography and Physical Environment

Yuri Korchagin field located in the Russian sector of the Caspian Sea. The distance to the nearest coast (Volga River Delta) is about 120 km. The nearest seaports are located in Astrakhan (175 km) and Makhachkala (250 km); there are railway stations - in the cities of Astrakhan, Makhachkala, Kizlyar and Derbent [1]. Overview of the Russian sector in the Northern Caspian is presented in Fig. 1.1.1.

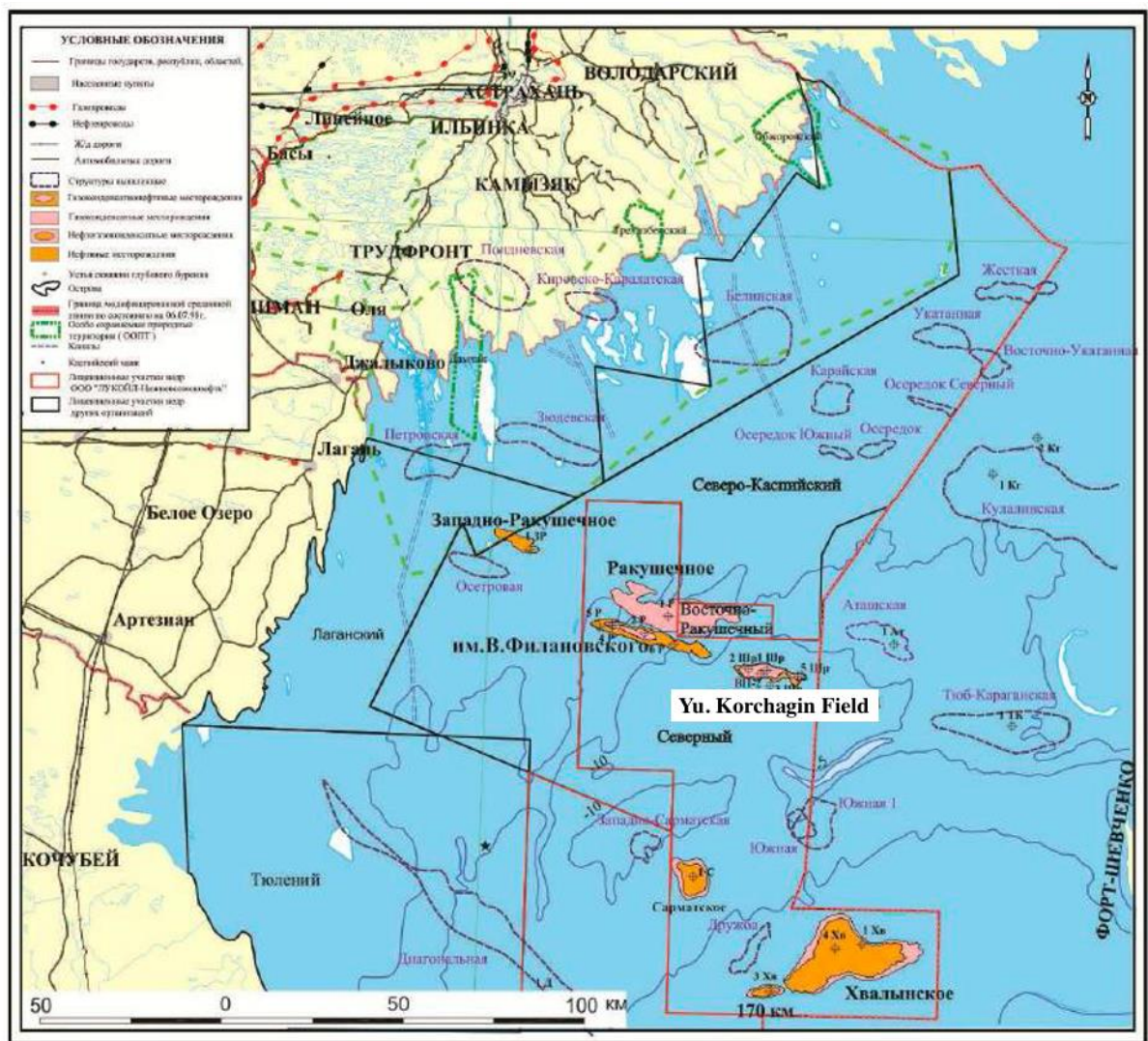


Fig. 1.1.1. Overview of the Russian sector in the Northern Caspian [1]

The Caspian Sea is the world's largest enclosed body of water. Historically, the issue of sharing water resources has been quite controversial. At the moment, a decision on the division of territories has been reached between Russia, Kazakhstan and Azerbaijan at the level of interstate agreements (2003), covering the North and Middle Caspian. According to averaged estimates [2], the hydrocarbon resources of the states of the Caspian region are distributed as follows: Kazakhstan - 48%, Russia - 19%, Azerbaijan - 16%, Turkmenistan - 11%, Iran - 5%. The sea is bounded by the Caucasus Mountains in the west and the steppes and deserts of Central Asia in the east.

130 rivers flow into the Caspian Sea, of which 9 rivers have a delta-shaped estuary. Large rivers flowing into the Caspian Sea are the Volga, Terek, Sulak, Samur (Russia), the Urals, Emba (Kazakhstan), Kura (Azerbaijan), Atrek (Turkmenistan), Sefidrud (Iran). The largest river flowing into the Caspian Sea is the Volga, its average annual drain is 215-224 cubic kilometers. The Volga, Ural, Terek, Sulak and Emba account for 88–90% of the annual drain to the Caspian Sea [3].

The area and volume of water in the Caspian Sea varies significantly depending on fluctuations in water level. At a water level of -26.75 m, the area is approximately 371,000 km², the volume of water is 78,648 km³, which is approximately 44% of the world's lake water reserves. The maximum depth of the Caspian Sea is in the South Caspian Depression, 1025 meters from the level of its surface. In terms of maximum depth, the Caspian Sea is second only to Baikal (1620 m) and Tanganyika (1435 m). The average depth of the Caspian Sea, calculated from the bathygraphic curve, is 208 meters. At the same time, the northern part of the Caspian is shallow: its greatest depth does not exceed 25 meters, and the average depth is 4 meters [4].

The water level in the Caspian Sea is subject to significant fluctuations. According to modern science, the total fluctuations in the water level in the Caspian Sea over the past three thousand years has reached 15 meters. According to archeology and written sources, a high level of the Caspian Sea is recorded at the beginning of the XIV century. Instrumental measurement of the level of the Caspian Sea and systematic observations of its fluctuations have been carried out since 1837, during which time the highest water level was recorded in 1882 (-25.6 m), the lowest - in 1977 (-29.0

m), s In 1978, the water level rose and in 1995 reached the level of -26.7 m, since 1996 there has again been a downward trend (Fig. 1.1.2.) [5]. Scientists connect the reasons for the change in the water level of the Caspian Sea with climatic, geological and anthropogenic factors.

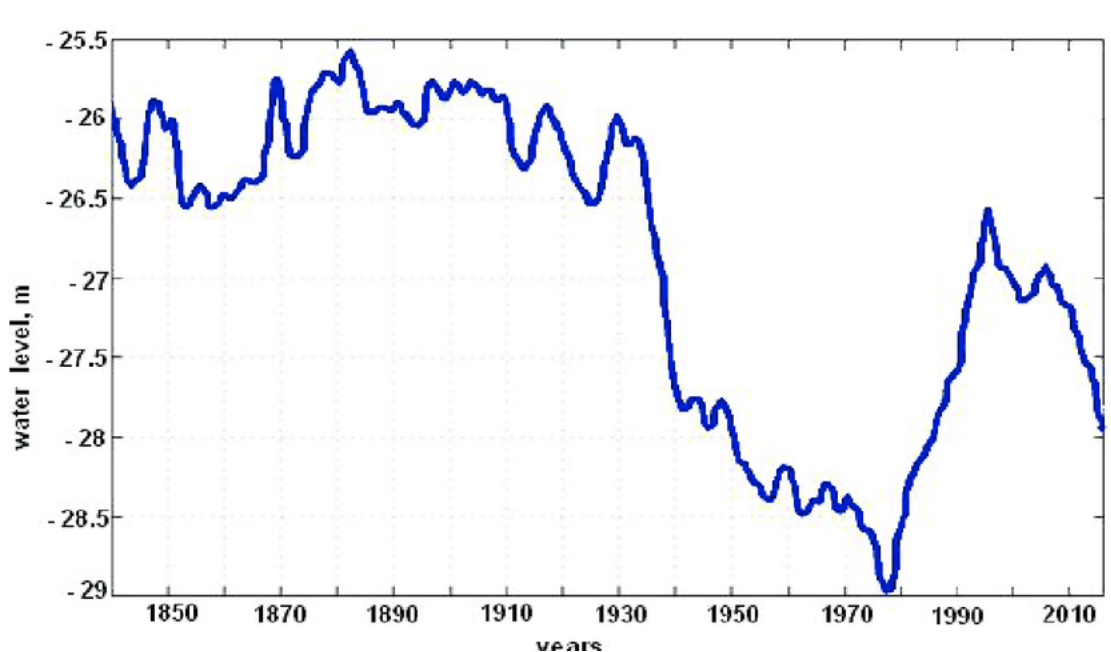


Figure 1.1.2. Dynamics of the water level of the Caspian Sea [5]

The continental climate prevails in the northern part of the Caspian Sea. In winter, the average monthly air temperature ranges from -8 to -10 °C, in summer - from $+24$ to $+25$ °C. The average annual rainfall is 200 millimeters. The average annual wind speed is 3–7 meters per second, northerly winds prevail. In the autumn and winter months, the winds increase, the wind speed often reaches 35-40 meters per second. The highest recorded wave height is 11 meters. The water depth in this area ranges from 11 to 13 meters. Summer water temperatures at coastal shallows can reach 25 °C or even more, but most of the north-eastern part of Caspian Sea freeze every winter [4]. The average surface temperature of the Caspian Sea is presented in Fig. 1.1.3.

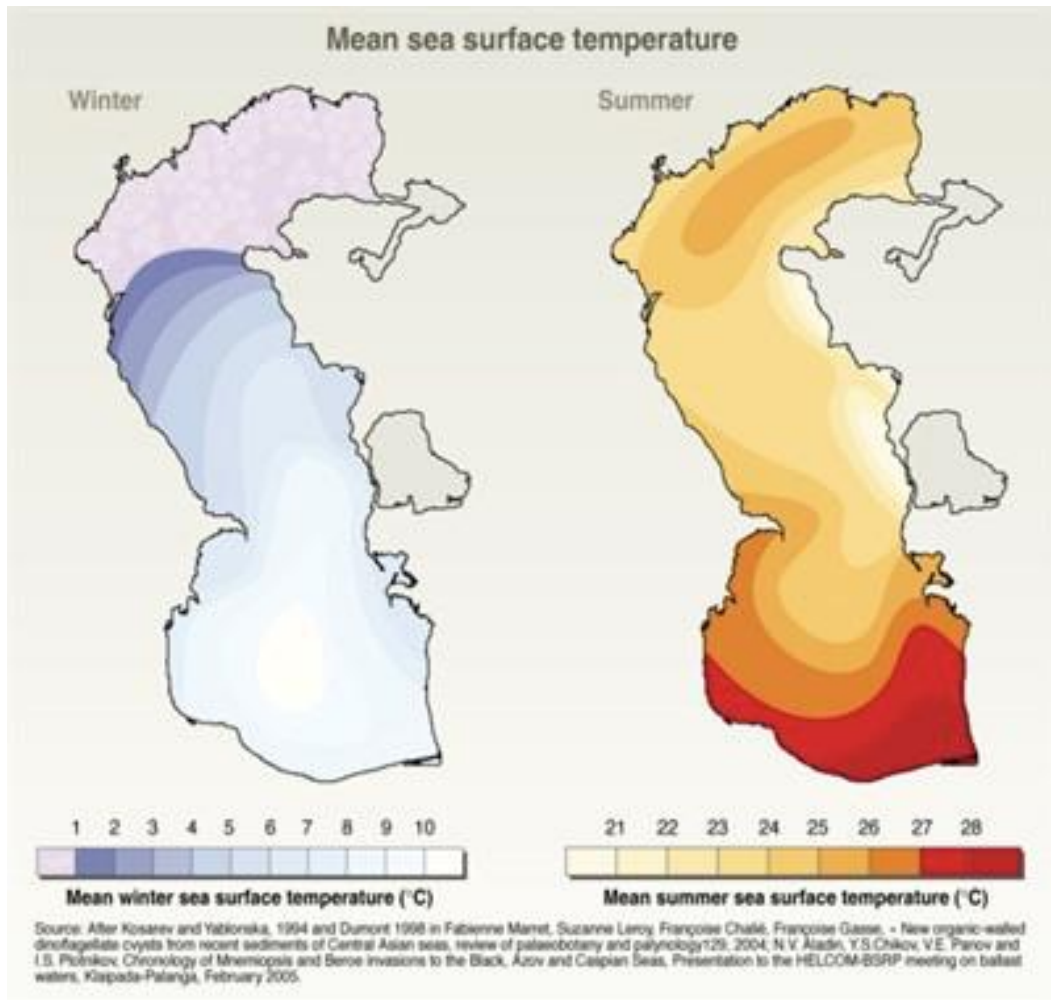


Fig. 1.1.3. Average surface temperature of the Caspian Sea [8]

Thus, one can conclude that the climatic conditions of this region are quite severe, and in winter they are comparable with Arctic conditions.

1.2. Geological Description

The Yu. Korchagin field is represented by two deposits - terrigenous sediments of the Lower Cretaceous age (Neocomian reservoir) and carbonate deposits of the Upper Jurassic age (Volga stage). The main industrial oil reserves are contained in the Neocomian reservoir, the area of which is 20.1 x 4.7 km, and the effective oil-saturated thickness is approximately 20 m. The position of the gas-oil contact of the Neocomian reservoir is noted at a depth of 1517.2 m, and the oil-water contact is 1537.1 m (Fig.

1.2.1.) [9]. Both productive horizons have significant gas and water-oil transition zones. In addition, reservoirs are characterized by heterogeneity in filtration properties, and the saturation pressure is close to the reservoir pressure. These factors cause a high degree of risk of gas/water breakthroughs in the intervals of the reservoir with high permeability and create the chance of the formation of stable gas and water cones. The operating mode of the reservoir is characterized as water-driven with the gas cap drive.

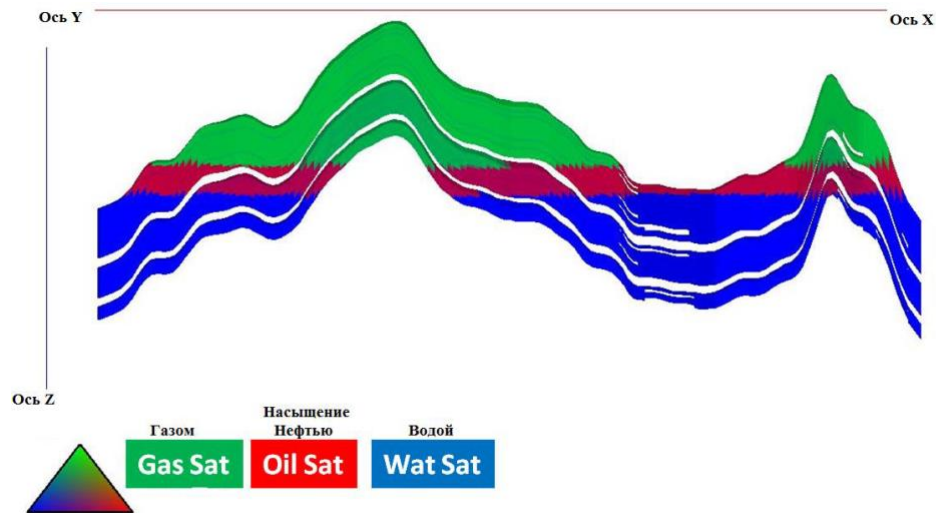


Fig. 1.2.1. Geological profile of the Neocomian stage [9]

As new information is gathered, geological representations of the object naturally evolves and is implemented into the geological model. The analysis of core material allowed to identify 6 lithotypes of rocks with stable dependencies: ‘PORO - S_{wcr} ’ and ‘PORO – PERM’: carbonated sandstones, sandstones and gravelites, intercalations of sandstones and clays, clays and siltstones, dolomites, limestones [10].

Based on them, with the exception of the carbonated sandstones, relationships were found with well logging data, which made it possible to use horizontal well data in a common information base, and the supplemented statistics made it possible to substantiate the variogram ranks for lithotypes with subsequent application of critical values to highlight reservoirs [10]. Comparative sections of the lithology cube of the initial and current geological and hydrodynamic models are shown in Fig. 1.2.2.

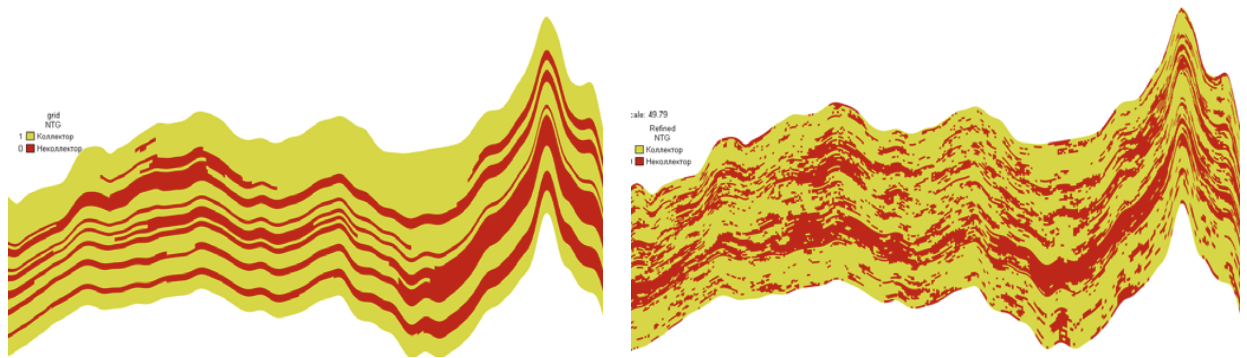


Fig. 1.2.2. Comparison of the initial and current sections of the lithology of the geological and technological model [10]

The Neocomian reservoir consists of lower, middle and upper members (1st, 2nd, 3rd members), represented by marine deposits formed by sandstone, silt and clays with thin interlayers of calcareous sandstone. Lower and middle Neocomian members predominantly consist of siltstones and sandstones of varying degrees of granularity (from small to large), often well-cemented clays and limestones, composed during a period of relatively non-intense sea level change. The Upper Neocomian member consists of poor sandstone deposits of the coastal slope with fine-grained mica, potassium feldspar and glauconite quartz sand, interbedded with silt limestone, siltstone and carbonate rocks. The frequency of calcareous interlayers of various thicknesses and amounts increases from top to bottom. The presence of carbonates in the pore space has a negative effect on the reservoir properties of the pack. A wide range of reservoir properties is due to the mineralogical composition of the formation and a variety of grain sizes, whereby there is a change in the porosity range of 12 to 23%, and permeability in the range of 1.0 to 145 mD [10].

The Upper Neocomian member has the least homogeneous lithological composition, where sandstone, occasionally interbedded with siltstone and clay inclusions, has the best reservoir properties. Some thin layers are cemented with lime cement. In the upper part of the section, it becomes coarse-grained and can pass into

granular limestone. The values of porosity and permeability vary in the range of 20-25% and 100-500 mD, respectively. It should be noted that the upper Neocomian member is isotropic, both in the vertical and horizontal directions.

In the middle and lower layers, anisotropy in permeability is observed, which is characteristic in the presence of clay interlayers. The reservoir is characterized by high porosity and permeability in the upper section with low permeability anisotropy. Gas saturation was observed over the entire area of the productive horizon, however, the flow capacity mainly depends on the relative permeability and gas saturation of the rocks, the permeability of which depends on the grain size.

One of the main difficulties associated with well placement and field development is the presence of a massive overlying gas cap and bottom water, where the oil rim has a thickness of only 20 m. In highly permeable formations with high vertical permeability, there is a risk of a decrease in oil flow from almost the first days of well operation, due to the formation of gas and water cones. The main task when placing the well was to drill a horizontal section of the wellbore at the maximum possible distance from the gas cap (about 15 m). This was necessary to avoid gas breakthrough and maintain the highest possible reservoir pressure required for oil inflow [10].

1.3. Physico-chemical Properties of Formation Fluids

The oil of the Neocomian reservoir and the Volga stage in reservoir conditions is light (density 807-810 kg/m³), low-viscosity (0.52-0.46 mPa•s), with a gas content of 107.8-118 m³/t. The pressure of oil saturation with gas is equal to the initial reservoir pressure at the gas-oil contact (GOC) and is 16.5-16.6 MPa. The mass content of resins in oil is 2.7%, asphaltenes 0.1%, paraffins 9%, salts 10%, solids 0.05%. The melting point of paraffin is 54 °C. The volumetric yield of fractions up to 100 °C is 6%, up to 200 °C - 28%, up to 300 °C - 52%, up to 350 °C - 66%.

The gas of the Neocomian reservoir and the Volga stage has the following properties: supercompressibility coefficient (z) - 0.89, volumetric coefficient - 0.00633, density in the reservoir conditions - 115.9 kg/m³, viscosity in the reservoir conditions - 0.013 mPa•s, heat capacity - 60.5 J/°C; molecular weight - 19.3 g/mol. The reservoir gas consists of: carbon dioxide 0.32%, nitrogen 1.46%, methane 89.14%, ethane 4.66%, propane 1.73%, isobutane 0.25%, n-butane 0.57%, isopentane 0.20%, n-pentane 0.27%, isohexane 0.15%, n-hexane 0.22%, the remaining components (from C7 or more) - 1.03%.

The gas condensate of the Neocomian reservoir and the Volga stage has the following properties: density (standard conditions) - 722 kg/m³, viscosity (standard conditions) - 0.54 mPa•s, molecular weight - 108 g/mol. The reservoir gas condensate consists of: carbon dioxide 0.11%, nitrogen 0.08%, methane 14.83%, ethane 4.24%, propane 4.63%, isobutane 1.68%, n-butane 5.2%, isopentane 3.29%, n-pentane 5.51%, isohexane 3.99%, n-hexane 7.38%, the remaining components (from C7 or more) - 49.06% [11].

1.4. Field development experience

The field was put into operation in April 2010 with a horizontal well drilled on the Volga carbonate deposits. Basic technological parameters of development of the deposit are shown in Fig. 1.4.1. The greatest attention is drawn to the dynamics of gas production, which characterizes the active involvement in the development of free gas reserves of the gas cap of the Neocomian deposits. In published articles (for instance, [12]) on the analysis of the development of the field, it is certainly mentioned that the design and actual productivity of oil wells are consistent with the dramatic discrepancy between the design and actual indicators of the gas-oil ratio and the growth rate of the gas factor, which led to a direct impact on oil production. So, after 4 years of operation, with relative compliance with the design and actual rates of drilling and commissioning, the level of oil production at the field was less than 60% of the planned level amid growing gas factor.

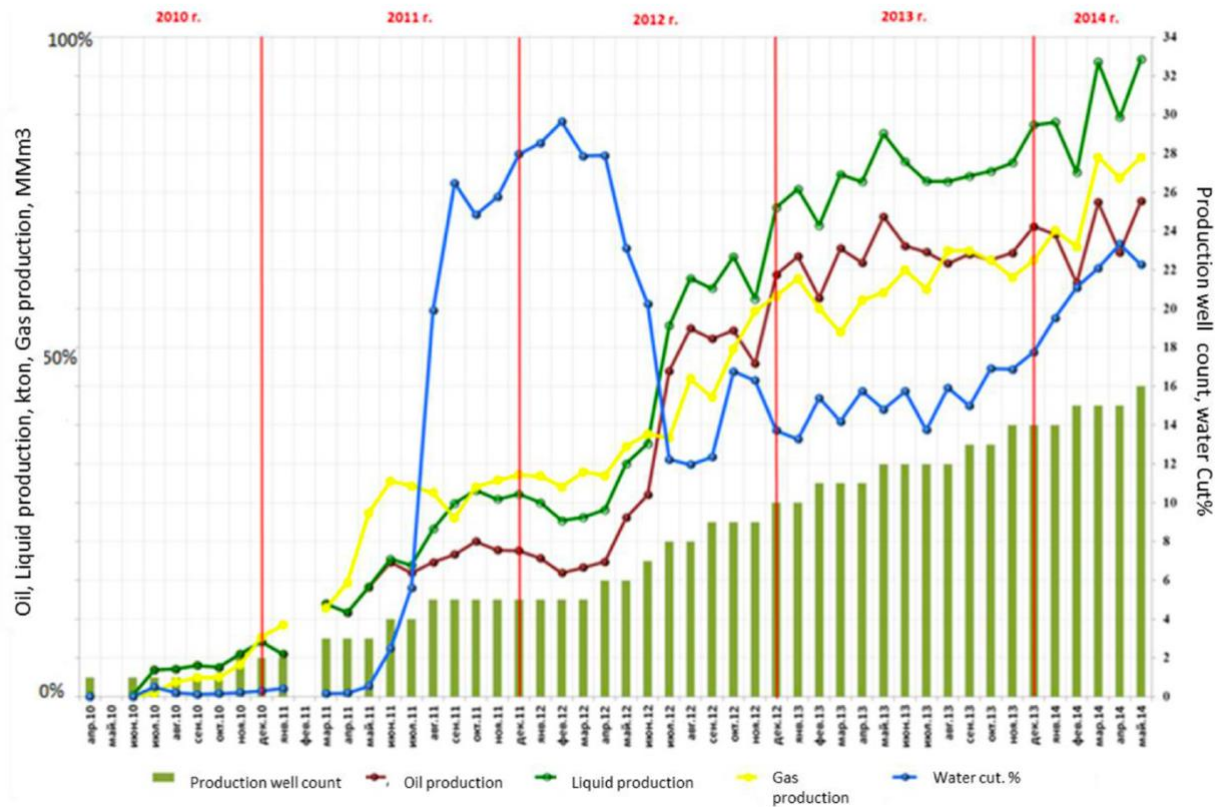


Fig. 1.4.1. Main technological parameters for the development of Yuri Korchagin field [10]

At the first stage of the project implementation, the uncertainties for the considered field can be reduced to the following ranked list:

1. Design parameters of drilling;
2. Well productivity;
3. Efficiency of well completion design;
4. Design solutions for surface equipment;
5. Uniform recovery of the reserves;
6. Gas and water cresting conditions;
7. Gas cap activity.

The influence of the gas cap on the development parameters was determined to be insignificant, firstly, due to the general low exploration of the field at the design stage (3 exploration wells) and, secondly, due to the ‘layered’ concept of the reservoir

structure, within which the main gas volumes were considered separated from the oil-saturated part of the reservoir.

The work of the first wells on the Volga stage was accompanied by technological complications (imperfections in drilling and completion), which made it difficult to draw conclusions regarding the correctness of the chosen geological concept.

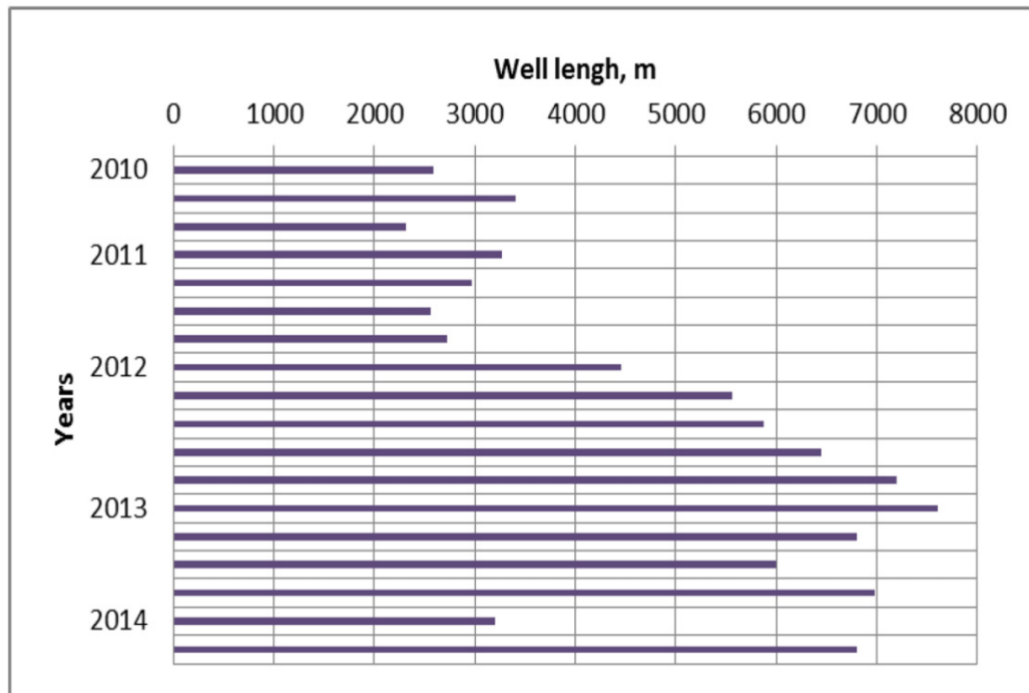


Fig. 1.4.2. The lengths of horizontal wells drilled in the Yu. Korchagin field throughout the period of the development [10]

The first work was carried out in terms of geomechanical modeling; adjusting the speeds and parameters of drilling and equipment used; modernization of well design and selection and testing of well completion systems. At the same time, a field work program was carried out to analyze the possible causes of reservoir behavior (tracer injections, well tests, production logging). A deliberate change in the drilling schedule with the primary commissioning of relatively short horizontal wellbores (2300-3200 m) to build up production and technological experience allows to confidently implement well drilling up to 7600 m long (Fig. 1.4.2.) [10].

1.5. Complicating Field Development Factors

The main and obvious the Yu. Korchagin field development problem is the gas breakthroughs from the gas cap into production wells. This is facilitated by high gas mobility compared to oil and a large reserve of potential energy.

Yu. Korchagin field offshore location is an additional complicating factor in its development. The development and operation of offshore fields is much more complicated and costly than onshore fields. The produced fluid, as a rule, has to be processed on a platform. Environmental requirements are significantly stricter than onshore. All this led to significant development costs.

In addition, the Yu. Korchagin field is located in a region with an unsteady seismic regime. It is influenced by: from the south-west - Makhachkala, and from the south-east - Mangyshlak seismically active zones, where earthquakes reach 6-8 points, and in the epicenter - over 9 points on the MSK-64 scale. According to the Joint Institute of Physics of the Earth of the Russian Academy of Sciences (IPE RAS), the seismic hazard of the work area is 4-5 points. The intensity of seismic activity decreases from southwest to northeast. Background seismicity on the MSK-64 scale once every 100, 500 and 1000 years is 4, 5 and 6 points, respectively.

Chapter 2. The technical part

2.1. Technical facilities at the Yu. Korchagin field

In 2005, the Central Design Bureau "Coral" made a feasibility study for the first series of offshore ice-resistant fixed platforms, intended for use at the Yu. Korchagin field. Having analyzed many options for alternative platforms, the Lukoil company made the final decision on choosing a complex of platforms, consisting of:

- Operating platform (IRP-1) with a drilling rig, as well as processing and power supply facilities;
- Platform with accommodation module (IRP-2);
- Catwalk;
- Single buoy mooring with soft connector;
- Floating oil storage;
- Subsea pipeline.

The complex of marine structures at the Yuri Korchagin field is presented in fig. 2.1.

Also, as part of the second phase of field development, construction of a satellite platform is envisaged to develop the reserves of the eastern part of the field. The construction of the satellite platform was completed in 2018.

Despite the fact that the total cost of the proposed complex with two platforms is about 18% higher than the alternatives, it was decided to use this concept, firstly, to ensure greater safety of personnel and, secondly, to ensure more comfortable living conditions on the platform. The complex consists of two independent platforms, one of which is a production complex, fully equipped with appropriate technological and energy equipment, and the other serves as a living quarters, fully equipped for optimal comfort and relaxation (including emergency power plant). It is assumed that this system, consisting of two platforms, does ensure the highest-level safety of working personnel that can be achieved in conditions work at sea.

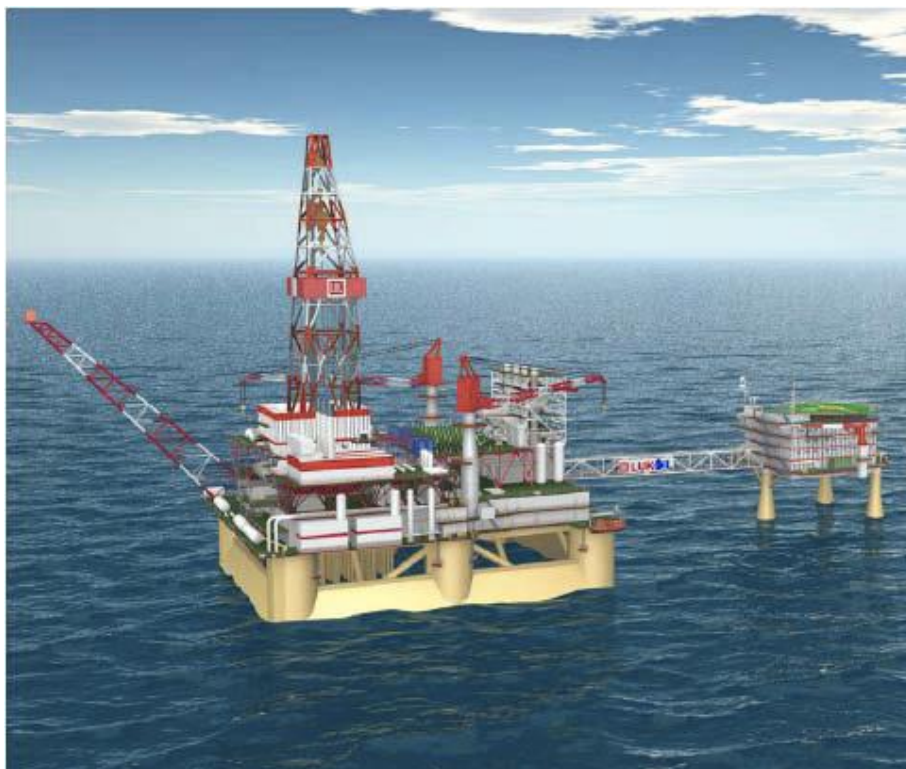


Fig. 2.1 Complex of offshore facilities of the Yu. Korchagin field [13]

The hull of the semi-submersible platform Shelf-7 is used as the foundation of the “working” platform, while the living module is located on a new ice-resistant base, consisting of a triangular pontoon and three legs. Each platform is pile supported.

Environmental issues have been determining factors in the analysis of potential design decisions, as the Yu. Korchagin field is located in the conservation area of the Northern Caspian. In order to ensure environmental safety and reduce the negative impact on the marine environment, the most modern principles, methods and means are implemented, such as:

- "zero discharge" principle;
- fish protection measures;
- industrial and environmental monitoring.

The enterprises of the «Caspian Energy» Group (LLC «CNRG») took direct participation in the creation of most of these objects. OJSC «Central Design Bureau Coral» carried out the development of design and engineering documentation for the IRP-1 working platform and the IRP-2 accommodation platform. Moreover, the design was carried out at all stages from the feasibility study of the project to development of

operational documentation. Also, other enterprises of the LLC «CNRG» Group, led by the Center for Marine Technology «Shelf»: OJSC Design Bureau «Vympel» (Nizhny Novgorod), «Astramarine» CJSC (Astrakhan), as well as Shipbuilding Design Bureau «The Caspian» (Astrakhan) took direct participation in the development of the design, engineering and technological documentation.

The entire construction cycle of IRP-1 and the manufacture of the supporting structure of the single buoy mooring were performed by the Astrakhan shipbuilding company with subcontractors. The enlargement of the support base and the upper structure of the IRP - 2 was also carried out at the production site of the enterprise.

The Crane Marine Contractor Company has completed river and sea transportation operations and on-site installation of IRP-1. Floating cranes installed and fixed the supporting base and the upper structure of the IRP-2 with piles.

The stationary platform IRP-1 is designed for drilling, wells operating, gathering and processing of produced fluids. A drilling complex with a lifting capacity of 560 tons was installed on IRP-1 for drilling wells with a maximum wellbore length of up to 7400 m. The platform is also equipped with two cranes with a lifting capacity of 70 tons. The length of the platform is 95.5 m, the width is 72.2 m. The height of the IRP-1 from sea level is 86.6 m. The weight of the platform when standing on the ground with liquid ballast is 25 655 tons [14].

High-tech equipment of the platform is designed to prepare processed oil and ensure its transportation through subsea pipelines to a floating oil storage facility. It provides for the collection, preparation and injection of associated gas into a gas injection well, and then the supply of oil gas to a transport subsea pipeline for delivery to the main onshore facilities. The project also takes into account the intake of gas from the Khvalynskoye field.

When designing the IRP-1, many new problems of varying complexity have been identified. Ways to solve some of them have become decisive for the project.

One of these tasks, for example, was the placement of living quarters on the platform. The upper part of the IRP-1 has a lot of very tightly placed oil treatment equipment (Fig. 2.2). Consequently, the placement of living quarters on the same

platform created serious difficulties in ensuring the safety and comfortable living conditions of the crew. Despite the fact that the location of all the complexes in the upper part of the platform ensured compliance with the requirements of regulatory documents on industrial safety, it became obvious that the removal of the living quarters outside the IRP-1 was an urgent need. Considering the positive experience of designing the Coral Design Bureau “D-6” platform in the Baltic Sea, it was decided to build a free-standing stationary platform IRP-2 with a living quarters for 105 people.

The development of the LSP-2 project turned out to be no less difficult. When choosing its architectural and constructive type, the features of the production base for the manufacture and installation of platform elements, ice operating conditions, as well as the characteristics of the selected shipping channels of the Volga River and the Caspian Sea Canal, limiting vessel draft during transportation to 4.2 m, were taken into account.

Living quarters, public, medical, and office premises, a galley block, and provision storerooms located on IRP-2. Living quarters are designed for 105 persons. A helipad is installed on the fifth deck of the IRP-2. The height of the IRP-2 from sea level is 38 m. The length of the platform is 41.5 m, width - 40.2 m [14].

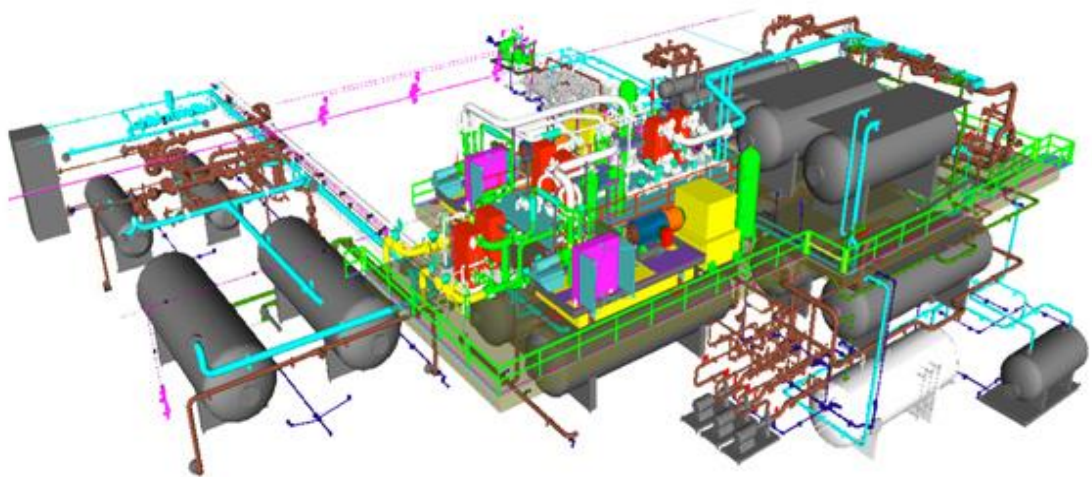


Fig. 2.2 Schematic representation of the oil treatment installation [15]

When designing both platforms, all the features of the area of the upcoming operation were taken into account, in particular the fact that the Yu. Korchagin field is located in a zone of difficult ice conditions that determine the external loads on offshore structures. Thus, the design of the IRP-1 and IRP-2 platforms was determined primarily by their ability to withstand the ice loads. So, during the implementation of the project it was decided to use the hull of unfinished semisubmersible drilling rig Shelf-7, adapted for ice conditions. The ice conditions also had a decisive influence on the development of the substructure of the living quarters.

To reduce the effect of the impact of ice loads on the IRP-1, the specialists of the Coral Design Bureau calculated and adopted the option with an ice fence along the entire perimeter of the platform with a heated face equipped with an angle of inclination to the horizon of 66° . The stability of the IRP-1 on the ground is provided by a pile mount, the structural elements of which are installed on the outer sides of the pontoons.

2.2. Ice model tests of IRP-1

In addition to the analytical method for determining ice loads, a test of the IRP-1 model was carried out in the Krylov ice basin. These tests were conducted to explore the interaction of IRP-1 platform with ice at small water depths.

The model investigations were carried in the ice basin with dimensions $40 \times 6 \times 18$ m, at a scale model test of about 1:60. Fig. 2.3 shows a general view of the IRP -1 model. The tests were carried out in three positions of the platform model: when the ice moves perpendicular to the length of the platform, perpendicular to the width of the platform and when moving diagonally. Next, the case of the position of the platform, when its length is perpendicular to the direction of ice movement will be considered, since in this case, maximum platform loads are assumed. In this case, the width of the platform along the waterline is 72.2 m at water depths of 14.9 and 12.2 m and 74.8 m at water depth of 7.8 m [13].

Investigation of the processes of interaction between offshore installations and drifting ice formations can be implemented in two ways: by towing a model rigidly

fixed to the towing carriage through an ice field (reverse movement mode), or by bypassing the ice field on a stationary installation model (direct mode movement) corresponding to real conditions. To study the influence of research modes on the process of ice accumulation and on the ice load values, some experiments were carried out in both modes. In these cases, the same ice conditions were simulated (ice geometry, strength characteristics and drift velocity), as well as water depth.

A special imitator of the seabed was used to study the effect of sea depths on the processes of interaction between the platform and ice. The simulator was made of tentless waterproof plywood, and its dimensions were chosen so as to provide sufficient area for the formation of ice accumulations in front of the platform. The roughness of the seabed and irregularities were not taken into account during the experiments: the seabed was presented as a flat surface.

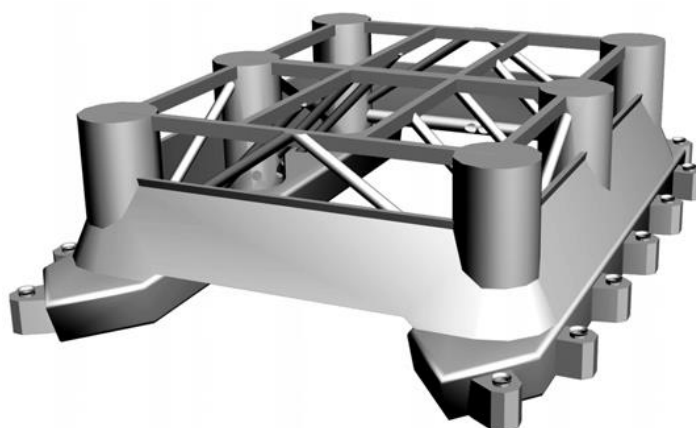


Fig. 2.3 General view of IRP-1 model [13]

Fig. 2.4 shows a schematic view of an experimental setup used in direct motion mode.

In the case of both direct and reverse modes of movement, the seabed imitator did not come into contact with a model rigidly mounted on a dynamometer. A small gap between the seabed and the model was made by cutting the bottom of the model to a height equal to the gap. A seabed imitator mounted on a carriage was towed along with the model. Loads acting on the seabed were not recorded. The experimental task was to measure ice loads only on the model of the structure at a certain water depth.

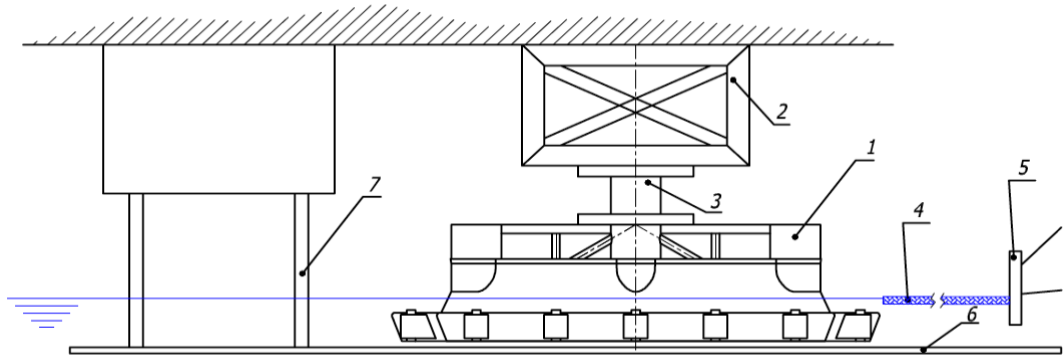


Fig. 2.4 Experimental setup for direct motion test: 1 – IRP-1 model; 2 - fixed frame; 3 - dynamometer; 4 – modeled ice; 5 - ice pusher; 6 – seabed imitator; 7 - supports for the seabed imitator [13]

Table 2.1 shows the data from the test modes and the measured maximum horizontal ice force acting on the platform.

Table 2.1

Test modes selected for analysis [13]

№	Ice thickness [m]	Water depth [m]	Test motion mode	Amount of ice drift [m]	Force [MN]
1	0.8	12.2	Direct	200	39
2	0.8	7.8	Direct	350	59
3	0.8	12.2	Reversed	450	42
4	0.8	7.8	Reversed	450	51
5	0.6	12.2	Reversed	400	20
6	1.2	12.2	Reversed	900	84
7	Ridge	12.2	Direct	350	44
8	Ridge	7.8	Direct	300	63

The hummocked ridges modeled in the experiments correlated to natural hummocked ridges featuring a 0.8-m-thick consolidated layer and 5.3-m keel depth.

The experiments were carried out at an ice drift speed of 0.5 m/s and a flexural strength of 0.6 MPa.

Fig. 2.5 shows the process of ice rubble accumulations forming at the base of the platform during ice movement. Table 2.1 contains the information about ice drift amount for each test. The test duration was determined by the condition for achieving a stationary interaction process when:

- the ice rubble had achieved a streamline contour;
- ice breaking had transferred to the outer boundary of the rubble;
- mainly broken ice streamed past the structure in the horizontal plane.

After completion of a test run, the level ice in the vicinity of the rubble pile was carefully removed to estimate the size of underwater ice formations in front of the platform. The moment when the ice touched the bottom was fixed using a video camera or a special rod.



Fig. 2.5 Forming ice rubble accumulations in front of IRP-1 model [13]

One of the tasks of the experimental research was to compare the experimental results obtained by implementing both modes under the same conditions. Fig. 2.6 shows the time dependence of the horizontal load acting on the platform model during experiments 1 and 3. As can be seen from this diagram, the records indicate a rather close correlation not only in the loads, but also in the frequency of the processes. The drops in the diagram correspond to the situation when the surface layer of ice near the platform fell under water, which led to a sharp decrease in loads. The result obtained

is of great practical importance, since it allows one to choose an experimental plan that is best suited for studying the interaction of structures and ice.

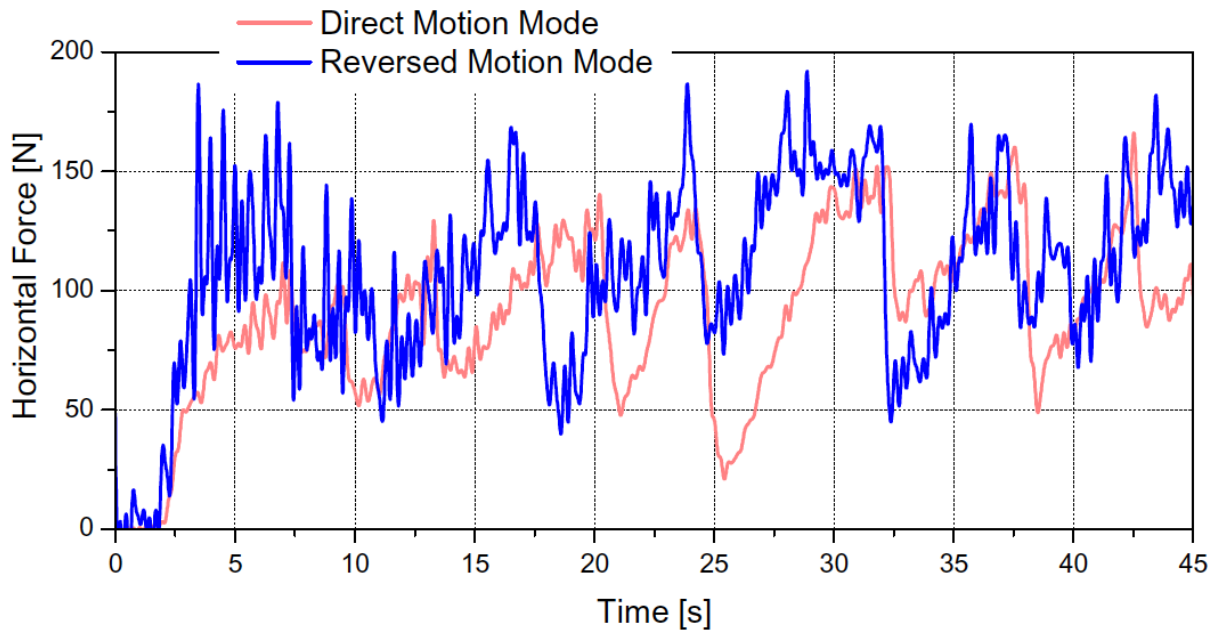


Fig. 2.6 Comparison of time histories obtained in both direct- and reversed-motion modes [13]

Runs 2 and 4 differ from runs 1 and 3 in the interaction of the underwater part of the ice fragments and the imitator of the seabed. Looking at the diagram in fig. 2.7 (run 2), it can be seen that the horizontal load reaches its maximum value at the initial stage of interaction of ice with the bottom, when the underwater part of the ice only touches the seabed, but are not fixed to it. As ice formations develop, the seabed begins to take on some of the load, while the processes of ice destruction are shifted to the outer boundary of the ice accumulations, and the line corresponding to the values of the load peaks gradually decreases.

Ultimately, the obtained experimental data showed that the platform foundation provides reliable protection of existing structures from ice loads.

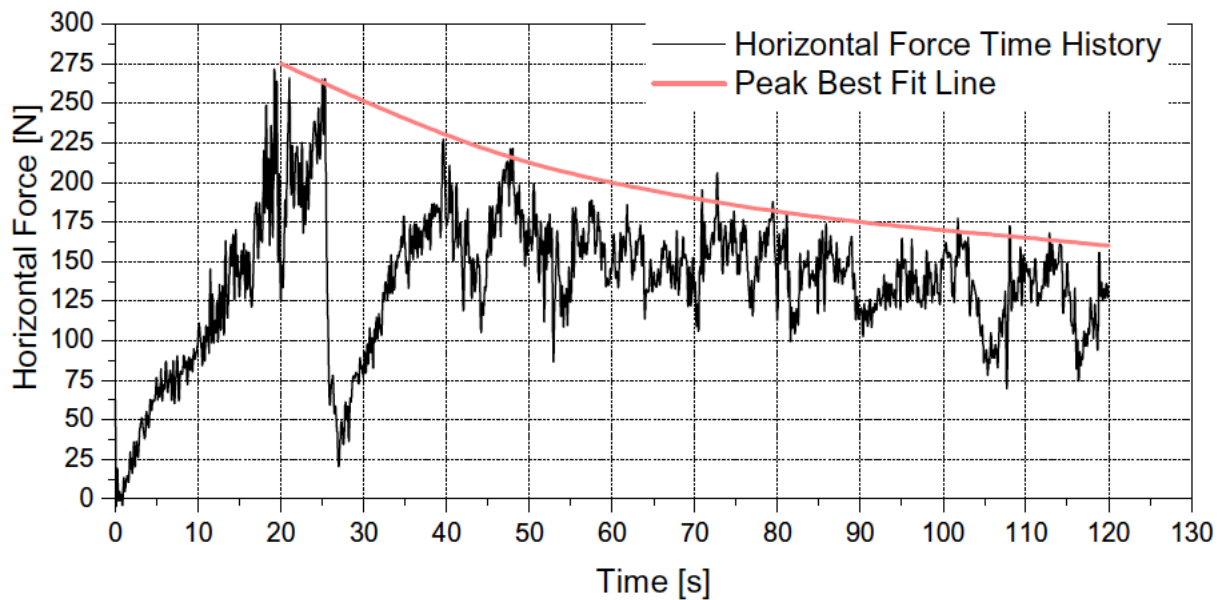


Fig. 2.7 Horizontal ice-force time history and peak best-fit line in case of formation of grounded rubble. [13]

2.3. IRP-1 and single buoy mooring construction

IRP-1 and a buoy mooring with a soft connection were built directly at the Astrakhan Shipbuilding Production Association (ASPA) plant. The living quarters and its foundation (IRP-2) on the ASPA slipway were prepared from more than twenty transport elements into two blocks, which were subsequently shipped and mounted on the field.

The construction of IRP-1 was carried out in several stages, each of which was unique in its own way and allowed the staff of the plant and related organizations to accumulate extensive experience in the formation and installation of large-sized block modules.

The first stage of the work was the dismantling of equipment and pipelines, the use of which was impossible, as well as metal structures that did not fit into the new design of the installation. At this stage, as part of the production preparation, all the necessary conditions were created for work directly on the platform:

- the floating facility was provided with electricity within 22 MW;
- a system for delivering personnel to a mark of 30 m and above was created;

- the compartments were properly ventilated and heated;
- a “Southern” slipway directly adjacent to the gates of the hull workshop, where the main large-sized blocks were subsequently built, was created.

The created conditions made it possible to conduct round-the-clock work around the entire perimeter and height of the facility and attract up to 1300 people per shift to the construction work [16].

Particular importance in the performance of work was given to labor protection, industrial and environmental safety.

The first stage of construction consisted in the manufacture and installation of the ice protection metal structures and pile mount brackets with a total weight of about 2 thousand tons. Their uniqueness was in the use of high-strength steels, as well as in the design of ice protection, which is heated to increase efficiency. It is implemented by integrating coolant circulation channels into the supporting frame of the ice protection sections. The construction of a structure of such complexity posed a challenge to the production, which could only be solved by developing a special technology for welding sections and tight control over its implementation. The successful solution of this problem is confirmed by the performed tests for tightness of the design of the heating channels located around the perimeter. For the manufacture of ice protection, a large-block construction method was used. Installation of sections of ice protection weighing 250-300 tons was carried out by the «Bogatyr-3» floating crane (Fig. 2.8), owned by the Crane Marine Contractor.

The large-modular installation method was also chosen for the subsequent stages of the construction of the entire platform because of tight construction time. It consisted in the manufacture and repletion of independent load-bearing modular structures, the construction of which was carried out at separate sites. This method made it possible to carry out work in parallel, the simultaneous execution of which on the platform would be impossible, and thereby reduce the construction time. Using this method modules were built, each of which was a separate complex as part of IRP-1 (drilling, energy, production complex, etc.). The modules were as complete as possible with equipment, piping systems and cable routes. The weight of one module could reach up

to 800 tons. Installation of such modules on the platform was carried out by a floating crane "Volgar" with a lifting capacity of 1600 tons (Fig. 2.9).



Fig. 2.8 Floating crane «Bogatyr-3» [17]



Fig. 2.9 Floating crane «Volgar» [18]

Large-module construction required modernization of the production. For this purpose, a complex was built at the enterprise which includes two concrete

construction sites and a mooring wall 100 meters long with the possibility of mooring floating cranes and transport floating objects. The concrete construction sites (2250 m² each) are equipped with a system of ship rail tracks and have a bearing capacity of 50 t/m² [16].

Other problems that the manufacturing plant had to solve were no less difficult. One of them was the construction of movements inside the moonpool complex on the platform. It is a support frame mounted on rails, along which the moonpool moves. In addition to the use of high-strength steel, the construction of this complex also imposed stringent requirements on the geometry of the structure. The tolerance for deviation from the general flatness level of the support belts was not more than 5 mm by 25 meters with overall dimensions of 27x13x2 m and a weight of the structure of about 100 tons. To maintain the specified tolerance, it was necessary to develop separate technology for welding the support frame when assembling it into a volume and special measures involving the machining of support belts. As a result, the construction of the moonpool with a total weight of about 1 thousand tons got the opportunity to move with the help of powerful hydraulic cylinders, serving all 33 wells [16].

For the final stages of the construction of the IRP-1 at "ASPA" (commissioning and testing) an appropriate project was developed. These stages included checking the strength and density of all systems, supplying power to all consumers, and putting into operation equipment and systems that ensure the safety and survivability of the IRP-1 when it is transported to site and placed on the ground. One of the main elements of the tests was getting the confirmation from the Maritime Register and the customer of the power plant operation under a full load of 22 MW.

The single buoy mooring was under construction at ASPA at the same time as IRP-1 (Fig. 2.10), which is part of the complex of the Yu. Korchagin field. During the foundation structures construction for the single buoy mooring, the production of shells made of high-strength steel with a thickness of up to 50 mm, a diameter of up to 2.5 m and a length of 30 m were mastered. Subsequently, a dimensional module with a mass of more than 800 tons and a height of more than 27 meters was formed. In this case, the welded joints were subject to non-destructive testing, including gamma rays, under

the supervision of DNV and an insurance surveyor. This task was also successfully solved, and the structure using the «Volgar» floating crane was shipped and subsequently installed at sea [19].



Fig. 2.10 Single buoy mooring [20]

2.4. Floating oil storage

The offshore transshipping complex includes a floating oil storage and a single buoy mooring. The complex is designed for oil offloading to shuttle tankers, which ensure the delivery of untreated oil from the Yuri Korchagin field to onshore facilities near the port of Makhachkala and further to the pipeline system of «Transneft». A floating oil storage facility consists of a double-bottom and double-side oil tanker, a machine-boiler room, a living structure and a helipad (Fig. 2.11).

The floating oil storage deadweight is 28,000 tons, length - 132 m, width - 32 m, side height - 15.7 m, crew - 25 persons. The buoy is intended for loading oil from an underwater pipeline into the oil storage facility and onto shuttle tankers. Oil from IRP-1 at the Yu. Korchagin field is delivered to the offshore transshipment complex via an

underwater pipeline with a length of 58 km and a diameter of 300 mm. The oil pipeline is laid along the bottom of the sea without being buried in the ground. The wall thickness of the pipeline is 16 mm [21].



Fig. 2.11 Offshore transshipping complex [20]

2.5. Satellite platform

The satellite platform is presented in the form of an offshore ice-resistant stationary platform (Fig. 2.12), designed for the development of offshore fields, and includes the minimum of necessary equipment. The satellite platform management is carried out from the IRP-1.

The satellite platform includes two main parts:

- upper structure with placed wellheads, main technological and auxiliary systems, helipad,
- sub structure with a pile foundation on which the upper structure is installed, which is also designed to protect marine conductors, risers and power cables against external loads.

The satellite platform is designed for drilling wells and field eastern part reserves development. In addition to the technological equipment, there are living quarters for the temporary stay of maintenance personnel, security systems and a helipad on the platform. The operation of the facility is almost completely automated - the crew consists of 8 persons. The produced hydrocarbons are pumped to the main platform through a system of subsea pipelines for preparation and subsequent shipment to the shore [23].



Fig. 2.12 Upper part of the satellite platform [22]

Chapter conclusions

Analyzing the technical part of the Yu. Korchagin field development project, one should note several main advantages of the chosen field development concept, such as:

- Separate placement of production and living modules. This concept provides the highest level of safety in working conditions at sea, and also provides a more comfortable accommodation for staff. This concept has successfully established itself

at the Kravtsovskoye field in the Baltic Sea, which was put into development in 2004, and subsequently was also used at the V. Filanovsky field on the shelf of the Caspian Sea;

- Local content in manufacturing. The main part of the design, construction, transportation and installation of the platform was carried out by Russian companies, mainly in Astrakhan city. This approach allows to reduce the production costs for the company, simplifies further maintenance of facilities, and also positively affects the state economy;

- "Zero discharge" principle. Today, the issue of environmental protection is one of the most significant in terms of hydrocarbon field development. "Zero discharge" principle involves the collection of all technological waste into containers and their subsequent removal to the mainland for subsequent processing. This approach allows to eliminate marine environment pollution.

Chapter 3. The technological part

3.1. Description of the current state of field development

On the basis of the authorized project document, oil and gas-condensate accumulations in the sediments of the Neocomian and Volgian stages are being developed at the Korchagin field. Yu. Korchagin field is started to be developed in April 2010. Sediments of Volga stage were put into production first. Commissioning of the technological complex for oil treatment was carried out in April-June 2010, full-scale hydrocarbon production has been underway since July 2010.

Development of Neocomian stage accumulations began in June 2011. Development of the field is carried out by wells with horizontal completion of the wellbore. Wells of the Volgian stage are equipped with perforated pipes, and wells of the Neocomian stage are equipped with sand filters. Information on the implementation status of the project's number of wells stock and the characteristics of the wells for 01.01.2020 are given in tables 3.1, 3.2.

As it can be seen from the tables below, drilling of the field was not completed by early 2020 and is being conducted close to the project. According to the plan, in order to minimize the geological risks associated with drilling of horizontal wells in the conditions of high geological uncertainty of the Neocomian stage, a uniform radial distribution is provided over the area of production wells with a horizontal wellbore coverage of up to 6.5 km near OWC, parallel to its surface.

At the same time, as stipulated by the project document, the trajectory of each subsequent well is specified not only by the results of the drilled wells, but also directly in the process of drilling in real time using geosteering equipment. This provides real-time monitoring of changes in the structural characteristics and formation composition of target objects. The obtained information is used to update the geological and geomechanical model for more efficient planning of the trajectories of subsequent wells.

Table 3.1

Implementation status of the project wells for January 1, 2020 [24]

№	Well stock category	Neocomian	Volgian	Total
1	Approved project wells, total	34	8	42
	Including:			
	-exploitation wells	31	6	37
	-injection wells	3	2	5
	-gas wells	-	-	-
	-monitor wells	-	-	-
	-water wells	-	-	-
2	Well numbers by 01.01.2018	31	7	38
	Including:			
	-exploitation wells	28	5	33
	-injection wells	3	2	5
	-gas wells	-	-	-
	-monitor wells	-	-	-
	-water wells	-	-	-
3	Wells to be drilled in 2020	2	1	3
	Including:			
	-exploitation wells	2	1	3
	-water-injection wells	-	-	-
	-gas wells	-	-	-
	-monitor wells	-	-	-

Table 3.2

Well number characteristics for 01.01.2020 [24]

Name of well stock	Well stock characteristics	Number of wells
Number of Producing wells	Drilled wells	33
	Wells were switched from other horizons	
	Total	33
	Including:	
	Wells in operation	33
	Inactive wells	-
	Wells development	-
	Suspended wells	-
	Wells were conversed to water-injection	-
	Wells were switched from other horizons	-
	Wells were conversed to monitor wells	-
	Abandoned wells	-
Number of Water-injection wells	Drilled wells	2
	Wells were switched from other horizons	-
	Wells conversed from production	-
	Total	2
	Including:	
	Wells in operation	2
	Inactive wells	-
	Wells development	-
	Suspended wells	-
	Under optimization	-
	Wells were switched to other horizons	-
Abandoned wells	-	
Number of Gas-injection wells	Drilled wells	3
	Wells conversed from production	-
	Total	3
	Including:	
	Wells in operation	3
	Inactive wells	-
	Wells development	-
	Suspended wells	-
	Wells were switched to other horizons	-
Abandoned wells	-	

The total number of wells drilled at the field is 38, of which 33 are in production, two water injection, three gas injection and four exploratory and appraisal wells (1, 2, 3, 5-Latitude). All producing wells are operated in a free-flow production method. Exploration and appraisal wells have been abandoned in accordance with the requirements of safety at sea.

Wells are distributed according to production zones as follows:

- For Volgian deposits – 5 producing and 2 water-pumping;
- On Neocomian deposits - 28 producing wells and 3 gas injection wells.

In contrast to the project document, regarding the re-injection of gas, it was planned to drill two gas injection well at the Neocomian gas cap, in fact two gas injection wells were drilled. The need for a third well (drilled in April 2015) was associated with an increase in gas volumes for re-injection due to a more intensive breakthrough of gas into production wells than expected, and the fact that the pressure at the wellhead G-1 reached the maximum allowable (15.8 MPa).

So, for 01.01.2018, the project total gas production (dissolved and breakthrough) was supposed to be 1 353 million m³, actually 2 816 million m³ of gas were taken, including 402 million m³ of dissolved and 2 414 million m³ of breakthrough gas. The cumulative volume of gas pumped into the Neocomian gas cap is 3 720.8 million m³ [25].

The results of a study of the gas breakthrough reasons and sources indicate that there is a closer hydrodynamic connection between the Neocomian and the Volgian deposits through possible decompression zones confined to the seal between them. First, mathematical modeling, and then the results of tracer studies, confirmed this. So, the presence of tracers injected with water into the VP-2 well (Volgian) and with gas into the G-1 well (Neocomian) was recorded in the producing wells 11, 12, 14, 110, 113, 107, 104 [25].

In August 2010, the VP-2 water injection well was commissioned to pump the extracted reservoir water into the water-bearing zone on Volgian deposits. As for 01.01.2018 the total volume of water pumped into the Volgian stage is 645.7 thousand

m³, including 30.2 thousand m³ of water taken from the aquifer of the Neocomian deposits of the Filanovsky field [22].

In general, 8 821 thousand tons of oil, 10 560.1 thousand tons of liquid and 8 568.1 million m³ of gas, including 682.8 million m³ of dissolved gas and 7 885.3 million m³ of breakthrough, were taken from the field over the entire period of operation. At the beginning of 2018, the gas factor was 950 m³/t, water cut of 19.7%, with average annual values of 1105 m³/t and 17.9%. The decrease in these indicators is due to the commissioning of new wells [25].

Initial recoverable oil reserves of 28,669 thousand tons were depleted by 30.1%. The current oil recovery factor is 0.095. The gas reserves of the gas caps of the Neocomian and Volgian deposits, amounting to 32.4 billion m³, were depleted by 14.2%. The field is constantly monitored for development, and a research program is being implemented [25].

3.2. Field development control

Development control should include the following set of studies/ data collection:

- 1) regular measurements of downhole and wellhead pressures across the entire number of production wells;
- 2) systematic measurements of flow rates, water content, and gas factor on wells;
- 3) conducting a complex of field geophysical research on:
 - determining the inflow and intake capacity profile;
 - identification of sources and intervals of gas and water breakthroughs;
 - inspection of the technical condition of the well;
- 4) conducting a complex of hydrodynamic studies for:
 - energy properties of the reservoir (wellhead, bottom-hole and reservoir pressure, pressure drop, productivity);
 - filtration properties of the formation (hydroconductivity of the far and near zone, permeability of the far and near zone, skin factor);

5) conducting a complex of geochemical studies on the study of deep and surface samples of fluids.

Currently all production wells are regularly monitored for production rates, water cut of produced fluids, and gas-oil ratio. Measurements of produced fluids are made using three-phase flow meters from Emerson and PhaseWatcher from Schlumberger [26].

Downhole and wellhead pressure measurements are continuously performed in all producing wells. Moreover, each producing well is equipped with a downhole sensor for measuring the bottom-hole pressure.

Monitoring of development by geophysical methods involves conducting the following studies in production wells:

- flow rate measurement - obtaining a reservoir inflow or injectivity profile at its individual intervals;
- thermometry - to identify working reservoirs, determine oil-gas-water flows, identify reservoirs with gas and/or water breakthroughs;
- moisture measurements - to determine the composition of the fluids in the wellbore, under favorable conditions - to determine the water cut (volumetric water content) in the production of wells;
- resistance measurement - to assess the composition of fluids in the wellbore, to identify intervals of water inflow, to assess the mineralization of water at the bottom of the well;
- densitometry - to determine the composition of the liquid in the wellbore, identify the intervals and sources of water flooding, establish the intervals of oil, gas, and water flow into the well in combination with flowmetry and thermometry methods for evaluating the operational characteristics of the reservoir.

Various domestic and foreign companies are currently offer sets of small-sized devices for field geophysical research of horizontal wells to conduct these studies.

Field geophysical research has already been conducted and is planned to be carried out in the future at the Korchagin field using the Schlumberger FSI (FloScan

Imager) device with the MaxTRAC traction system. The FloScan imaging system allows to determine the phase content of three-phase flow in the cross section and the velocity profile in real time. For two wells (11, 14), it was possible to build complete profiles of inflows according to the multiphase flow meter (FlowScanner), for two other wells (14, 110), integral estimates of phase flows were made [27].

Based on the latest advances in fiber-optic sensors, Sensa, a division of Schlumberger, has created innovative distributed temperature control systems (TCS). Using the TCS system in conjunction with downhole fountain valves, provides real-time flow control and regulation, which allows one to make real-time decisions to optimize well performance. TCS installations are especially recommended for use in «smart» well completion systems, as they are the only reservoir control systems that provide comprehensive information under the packer.

A monthly monitoring of optical fiber thermometry data is conducted in well 113 at the Korchagin field, which allows to distinguish the intervals of intensive gas inflow [23].

To improve control over the technological parameters of the wells, it is recommended to expand the use of fiber-optic measuring systems. The advantages of using fiber-optic measuring systems include the placement of all electronic equipment at the wellhead, which facilitates its modernization and maintenance. The specified system includes sensors for measuring pressure, temperature and its distribution, flow meters, which allow real-time monitoring of the technological regime of wells, identify deviations in oil production and measure the water content in the reservoir fluid. In addition, measuring fiber optic systems allow independent monitoring of each production interval and are a reliable telemetry tool in conditions of high production wells, high temperature and pressure.

Such monitoring systems are successfully used in the fields of the North Sea. An example is the Weatherford integrated telesystem for smart wells, which performs various types of measurements – thermobaric, multiphase flow rates, distributed thermometry, and multi-station seismic profiling on a single-core optical cable.

3.3. Field pilot works

Extensive gas-oil and oil-water zones in the deposits of the Yu. Korchagin field are limiting factors for the application of influencing methods to formation and bottom-hole zone, which increase the risks of water and gas breakthroughs to wells' bottom hole. For example, hydraulic fracturing is unacceptable, leading to the possible vertical cracks and premature contamination or water flooding of well products.

During development of the Yu. Korchagin field, one of the main problems is achieving a uniform profile in the horizontal wellbore, as well as limiting and isolating gas and water breakthroughs. Currently, all the production wells drilled for the main production formation, (Neocomian sub-layer), are equipped with the ResFlow system. It is a passive intellectual completion, involving the installation of several sand filters along the length of the horizontal wellbore, selected as based on the reservoir properties of the formation in each interval of the wellbore. The regulation of inflow is passive, since it does not allow to overlap the intervals of gas and water during the development process.

As a result of drilling, new geological and field information was obtained, which clarified the geological structure of the field.

The geological conditions for drilling the wells turned out to be more complex than expected. The main complicating factor of the Volga layer and Neocomian sub-layer is an intensive gas breakthrough in producing wells. The source of the breakthrough is gas from the Neocomian gas cap.

According to well logs, core and drill cutting studies between Neocomian and Volga deposits, it was revealed that there is a closer hydrodynamic connection through possible decompression zones confined to the cap. This was also confirmed by the results of tracer studies.

Therefore, in order to isolate the gas inflow, it is recommended that pilot works should be carried out with the use of foam systems or technical devices such as AICS (adapted inflow control systems).

It is worth to mention that there is practically no history of such projects in Russia. Therefore, the main source of data for the preparation of this recommendation was the project at the Oseberg field, Norway, implemented in 2003. In addition, data were available on the project of the Snorre field, Norway, where foams were injected in 2001 [22]. However, in this project foam injection was used not to cut off the gas entry slots but to equalize the displacement profile with water-alternated-gas (WAG) injection. So Snorre data can be used to a limited extent.

In the process of developing and coordinating the documentation for the implementation of these works, a number of questions arose and the risks were identified:

- possible bacterial infection of the formation under the influence of unprepared sea water;
- negative impact on the production process and production of substandard oil
- loss of physical properties and freezing of the reagent (surfactant) under the influence of negative ambient temperatures.

To address the issues, LUKOIL-Engineering LLC, in the framework of field pilot work support, has prepared a field pilot work program for testing foam systems to limit gas inflow.

The pilot project was conducted in 2015, when the acceptance tests of a new generation passive inflow regulation system — wireless filter with inflow regulation system with a gas flow limiter developed by VARMHOLMS LLC — were carried out. This device creates hydraulic resistance to the gas phase at a given level, while the flow rate of the liquid phase remains almost unchanged, which allows to reduce gas flow in the well. According to the results of testing in 2012 at the Kotovskoye field of OJSC RITEK, it was possible to reduce the gas factor by 10 times with applying low drawdown, and when applying high drawdown on the reservoir, the gas factor was decreased by 2.2 times [28].

To solve the problem of limiting the gas breakthrough in the production well 11 of the Volga layer, the second phase of equipment testing was carried out.

According to the results of modeling and calculations, a decrease in the gas factor by 2–2.5 times was predicted. Fig 3.1 presents a schematic diagram of this system layout in well 11 [29].

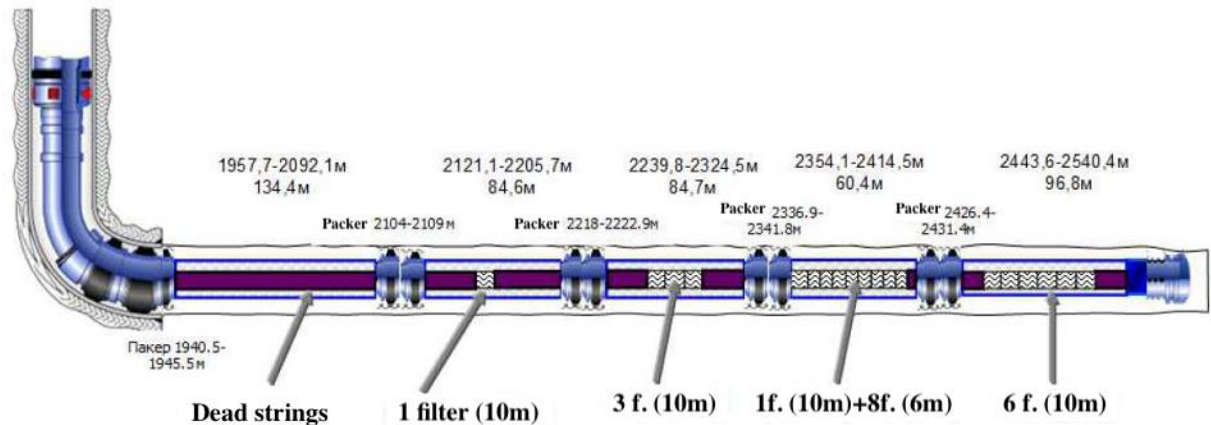


Fig. 3.1 Schematic diagram of the flow regulation system layout in well 11 [22]

By operator request "WORMHOLES" JSD has developed adaptive inflow control device (AICD) - that can adapt to changing characteristics over time, the inflow of liquid and / or gas phase.

The simplest version of the adaptive inflow control system is shown in Fig.3.2. It consists of a set of throttle rings with certain hydraulic characteristics and valves with a fixed shutter position (open or closed). Valves are manufactured to the required characteristics of AICD. This is achieved by means of the flow area of the valve seat and the stiffness of the valve plate, which provides the desired pressure drop of the valve to open or close it for a given flow rate.

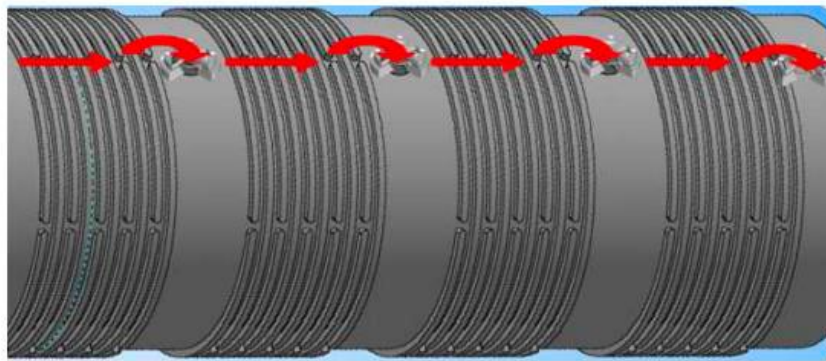


Fig. 3.2 Adaptive inflow control device option [22]

The work of the adaptive inflow control device is as follows: During the lowering, all valves are open. The flow of liquid and/or gas passes through the throttle ring and the open valve and enters the tubing. If a certain (set) value of the flow rate on the valve is exceeded, the valve closes. In this case, the flow path changes and the flow is directed to the next throttle ring. The hydraulic resistance of the system increases and the flow rate decreases. If the flow rate again exceeds the required value, the subsequent valve closes, etc. Such a system is the easiest to manufacture, but has a limited number of hydraulic settings.

One of the most important advantages of an adaptive system is the guaranteed presence of the system in a known position. The opening of all valves can be achieved by increasing the pressure in the wellbore. After that, the entire completion system is reconfigured for the changed production conditions. It is also possible to close any zone of the well by selectively increasing the drawdown during the injection of nitrogen through coiled tubing (flexible tubing) or tubing (tubing). In this case, spontaneous opening (closing) of the system is excluded without applying external opening pressure. It is also possible to launch partially closed completion equipment with the subsequent opening for the selective development of reserves, development of long wells and much more [30].

The proposed adaptive inflow control system can be used to solve the following problems:

- alignment of the inflow profile in horizontal wells;
- preventing cone formation in the heel area of a horizontal well;

- restrictions on inflow from zones with increased permeability or fracturing;
- water inflow restrictions;
- reduction in gas flow from breakthrough zones.

The uniqueness of the adaptive inflow control system is its ability to adapt to the changing conditions of the near-wellbore zone (flow intensity, clogging, etc.). Also, the system allows to limit the inflow from the interval at a certain level, which solves the problem of breakthroughs of water and gas. With complete water or gas breakthrough in a certain drainage zone, it is possible to completely cover this area, locally creating additional drawdown. In case it is required to open zones for inflow, it is enough to apply pressure from the wellhead.

Thus, the inflow control system makes it possible to adjust the optimal operation of the well using the completion system throughout the entire operation period.

After the planned test of the system at the Avilovskoye field, «Volgodeminoil» joint venture, the use of AICS was started at the Yu. Korchagin field.

The main objective of the application of inflow control systems is to align the inflow profile in horizontal wells, control production from zones with different reservoir properties, and delay the time of breakthrough of water and gas into the well.

One of the existing systems today is an active inflow control system with hydraulically adjustable valves that go down to the tubing inside the extension pipe (sand filter, perforated shank). Valves have the ability to adjust the level of plating of each zone from the surface.

To assess the effectiveness of the use of active inflow control systems, it was planned to use a similar system in the well №13 at the Volga layer drilled in 2013. The horizontal wellbore is 600-800 m long. Using an active inflow control system, it was possible to isolate individual zones in real time in case of a breakthrough gas or water. The schematic diagram of the intellectual completion of well 13 is shown in Fig. 3.3 [22].

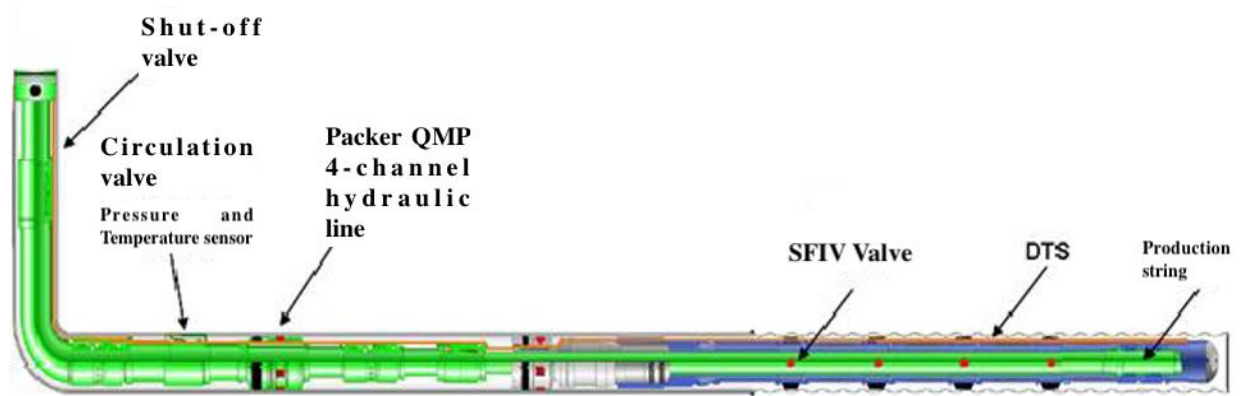


Fig. 3.3 The schematic diagram of the intellectual completion of well 13 [22]

It should be noted that modern active inflow control systems have a natural limitation on the length of the horizontal section associated with friction. The maximum length of the horizontal section for such systems should not exceed 4,200 m.

The disadvantages of active inflow control systems are the high cost of equipment, restrictions on the depth of descent, and a low degree of reliability of the equipment.

3.4. Analysis of the project document decisions implementation at the initial stage of development

At the Yu. Korchagin field, the development of oil and gas condensate deposits in the sediments of the Neocomian sub-layer and Volga layer is carried out on the basis of the approved project document. A comparison of actual and design development parameters for the entire field showed that in the period 2010-2012, actual levels of oil and liquid production were significantly lower than design parameters.

The main reasons for this significant discrepancy between the project and the actual parameters were as follows:

- a later start of reservoir development than planned. So, according to the project, the start of oil production was envisaged from 02/01/2010, in fact, the first oil was received in April, and the full-scale development of the field took place in July 2010. The actual number of producing wells at the end of 2010 (2 wells at Volga layer) was

less than the projected (6 wells) by four well, of which two were planned for the Volga layer and two for the Neocomian sub-layer. The geological conditions for drilling the wells turned out to be more complex than expected. The order of well commissioning was changed and commercial drilling speeds were reduced. Hence, the change in speeds affected the timing of construction and commissioning of wells;

- the actual average oil production rate of the Volga layer wells (275 tons/day) is 1.3 times lower than the projected (356 tons/day). This is mainly due to the lower permeability of reservoir rocks than predicted. Thus, the average permeability of the oil-saturated zone of the Volga layer in the updated reservoir model of 2013 is - 0.065 μm^2 (according to the project 1.65 μm^2). Secondly, because of higher gas factor than predicted (actual 694 m^3/t in comparison with project 126 m^3/t) due to a gas cap breakthrough [31].

Failure to comply with the plan for the associated gas utilization in 2010 (22%) is due to the fact that there was no provision for the procedure to implement into operation the design of the production and technological equipment complex with a small number of producing wells (2 wells) and during commissioning. In 2011, the actual production of oil and liquid (338.1 and 403.8 thousand tons) also turned out to be lower than the projected (1351.5 and 1435.6 thousand tons) by 75 and 72%, respectively. The reasons for this are as follows:

- the actual number of producing wells (5 wells) is lower than the design (9 wells) by four wells, of which one was planned for the Volga layer and three for the Neocomian sub-layer;

- average oil and liquid production rates in the field (280 and 335 tons/day) are lower than the design ones (515 and 547 tons/day), both for the reasons described above and due to the fact, that:

- the actual length of horizontal parts along the reservoir turned out to be less than the design one, which is explained by a more heterogeneous distribution of reservoir layers. So, for example, the production rate of well 110 was predicted at length equal to 856 m, and in fact it was 456 m;

- the actual water cut of the produced fluids (32.3%) for new wells of the Neocomian sub-layer exceeded the design (5.5%). The main contribution to the increase in water cut was made by the Neocomian well 113, in the production of which ~ 50% of water was noted from the very beginning of operation. This can be explained by the results of tracer studies, which indicate a closer hydrodynamic relationship between the oil-saturated and water saturated regions. In addition, the data of logging, core and drill cuttings indicate the absence in the interval of the bottom of the Neocomian sub-layer and the top of the Volga layer of cap with reliable shielding properties. Therefore, it can be expected that, within each of the deposits, impermeable layers can also be characterized by weak shielding properties and have zones of increased conductivity associated with zones of rock decompression or the presence of a fracture component.

- the gas factor continued to grow in the Volga wells, to an average of 2 097 m³/t, and the actual gas factor (290 m³/t) for the wells of the Neocomian sub-layer more than doubled the design (104.3 m³/t). Failure to plan for the use of associated gas in 2011 (92%) is due to the following. The actual gas factor for the entire field reached 1 460 m³/t (designed – 115.7 m³/t). In this regard, the molar mass of gas in the separation stages of the technological complex did not comply with design decisions. In order to prevent a decrease in the level of oil production during the commissioning period, the operator company was forced to limit the use of gas at levels 3 and 4. Following the completion of the commissioning of compressors, the level of associated gas use was increased from 40.1 to 99.3% [31].

In 2012, the actual production of oil and liquid (792.9 and 965.7 thousand tons) was lower than the projected (2347.5 and 2932.6 thousand tons) by 66 and 67%, respectively, due to the following:

- the actual number of producing wells (10 wells) is lower than the design (13 wells) by three wells, which were planned for the Neocomian sub-layer deposit;

- actual oil and liquid flow rates are 306 and 373 tons/day, which is almost 2 times lower than planned, equal to 595 and 744 tons/day, respectively. The main

reasons for the discrepancy between actual and design flow rates are similar to those described above.

The results of a study of the causes and sources of gas breakthrough, as mentioned above, indicate that there is a closer hydrodynamic connection between the Neocomian sub-layer and the Volga layer deposits through possible decompression zones confined to the cap layer between them. First, mathematical modeling, and then the results of tracer studies, confirmed this. So, the presence of tracers injected with water into the VP-2 well (Volga layer) and with gas into the G-1 well (Neocomian sub-layer) was recorded in the production of producing wells 11, 12, 14, 110, 113, 107, 104 [30].

3.5. Reasons of gas breakthrough and ways to minimize them

The uncontrolled breakthrough of hydrocarbon gases (HCG) into the oil rim of the reservoir can lead to a halt in well's production and incomplete production of oil reserves. It is believed that the horizontal sections of wells in most cases pass through a heterogeneous formation, which dramatically increases the likelihood of a quick gas breakthrough in unidentified highly permeable zones with increased fracturing.

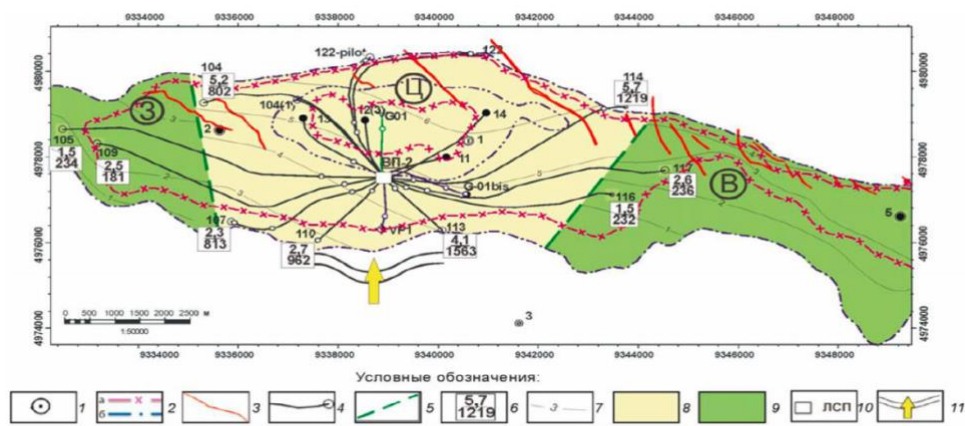
With the commissioning of horizontal production wells, accelerated (compared with the speed of the natural process) gas introduction into the oil rim is observed. According to available data, gas enters the rim from a gas cap of different ages, where, before the development of the deposit, excessive reservoir pressure was observed. Hence, at different sites, there are fluctuations in the levels of GOC deposits according to well logging data and testing in specific exploration and production wells. The uneven breakthrough of gas in different parts of the reservoir at the beginning of development led to the fact that the reservoir pressure is close to or equal to the oil bubble point pressure with a significant increase in the gas factor. The initial gas-oil ratio is about 120 m³/t for all wells under development, depending on a number of factors, it increases from 180.9 (well 109) to 1 564.8 m³/t (well 113). Thus, after the

start of oil extraction from the reservoir, an increasing process of reducing the thickness of the oil rim is observed [22].

When analyzing the factors of gas breakthrough into the rim, it turned out that certain characteristics (lithological-facies and petrophysical properties of the formation, oil saturation etc.) do not have a noticeable or regular effect on oil-gas ratios. Other characteristics show a general trend of increase in the oil-gas ratio (duration of production and, to a lesser extent, cumulative oil production in the well). The oil-gas ratio is influenced by such indicators as the height of the gas cap, the width of the reservoir, the gas factor (in dynamics), the density of oil, the concentration of hydrocarbons (density of gas reserves) and some others.

Among the listed reasons for the impact on the oil-gas ratio, the dependence on the inclination angle of the reservoir is considered below, which indicates an uneven reaction of the oil-gas ratio on the surface topography of the reservoir.

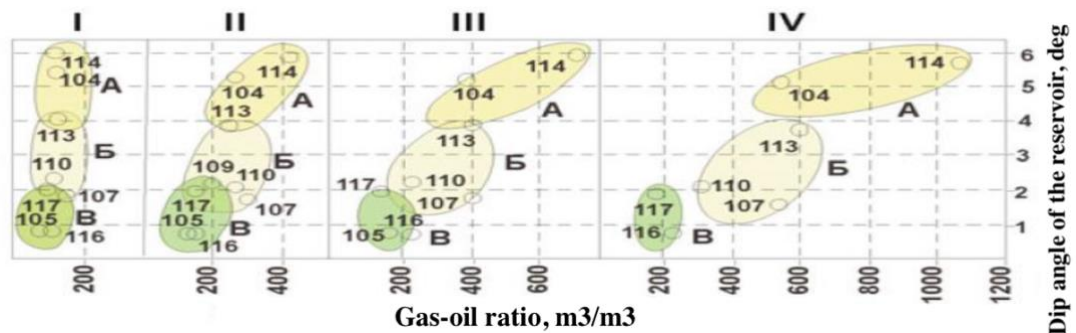
Depending on the angle of inclination of the reservoir, the field territory was divided into three parts: western, central and eastern, which are presented in Fig. 3.4.



1 - wells; 2 - contacts: a - gas-oil, b - oil-water; 3 - faults and shifts; 4 - the trajectory of the horizontal section of the well; 5 - boundaries of the blocks 3 - western, B - eastern, Ц - central; 6 - indicators of the reservoir inclination angles (numerator) and the values of gas-oil ratios (denominator); 7 - lines of equal values of the reservoir dip angles; 8 - the maximum values of the reservoir inclination angles and gas-oil ratios; 9 - the minimum values of the reservoir inclination angles and gas-oil ratios; 10- IRP-1 (ice-resistant platform); 11 - structural nose and place of admission of hydrocarbon gases to the central unit

Fig. 3.4 Oil-gas ratio values on the area of the field [22]

This dependence became more contrasting when considering the dynamics of well operation after 3, 6, 9 months (Fig. 3.5).



Groups of wells: in blocks: A + Б - central, Б - western and eastern; by dip angle of the reservoir, hail: A -> 3 °, Б - 2 ... 3 °, Б - <2 °; operation duration: I - starting position, II - 3 months, III -6 months, IV -9 months

Fig. 3.5 The dependence of the increase in the oil-gas ratio from the angle of productive deposits incidence and the time of the well operation [22]

In the central part of the reservoir, the dip angles are 3.0 ... 5.5°, the slope of the contours of equal dip angles is directed from south to north, with a sharp immersion on the northern slope of the reservoir (more than 5°). On average, in the central block, the value of oil-gas ratio is 1061.5 m³/m³. In the central block, two groups of wells are distinguished: northern (A) with an average value of the dip angle of 5.5° and southern (B) with an average value of the dip angle of 3°. In the central block, before commissioning, and regardless of the angle of incidence of the productive layer, the oil-gas ratio throughout its area retains the highest individual values and average values in the north and south. However, after putting into operation over time (especially noticeable after 9 months), the northern group of wells (A) of the central block with large dip angles has higher oil-gas ratio values than the southern group of wells (B) of this block with lower angles of the reservoir inclination. But there are no areas in the central block with low oil-gas ratio values, due to the maximum height of the gas cap, the universally high oil saturation and the concentration of hydrocarbons (density of gas reserves), and a number of other reasons.

Minimum oil-gas ratio values (average value is 243 m³/m³) are located to the west and east of the central part of the field, where the dip angles of the reservoir are 2° or less. The value of oil-gas ratio in these blocks is 4.7 times less than the value of oil-gas ratio in the central part. Particularly noteworthy is the fact that after

commissioning the wells of the western and eastern blocks and after 9 months of oil extraction, the oil in these parts remained practically in the initial position [22].

Small volumes of the reservoir with low oil-gas ratio values in the western and eastern parts of the field (compared with the central part) occupy a relatively small area. But these are precisely those parts where a large part of the rim oil reserves is concentrated and where at this stage of field development the minimal risks of increased gas introduction into the oil part of the reservoir.

There is another feature of the reservoir inclination that should be noted: with an increase in the angle of incidence, a decrease in the distance between the GOC and the wellbore is observed laterally. So, in well. 110 with an increase in the dip angle from 3 (286 m) to 6° (143 m), this distance is halved. In other words, the possibility of a gas breakthrough is higher where the dip is steeper and the distance from the well to the GOC is shorter [22].

In order to minimize the introduction of gas into the oil rim and determine the optimal trajectory of new production wells, it is recommended, in conjunction with other methods (for example, minimal pressure drops when developing a deposit with an existing number of production wells, new generation gas treatment facilities - gas breakthrough limiters), to concentrate the main production load in the lower half of the peripheral western and eastern parts of the rim, thereby restraining the growth of oil-gas ratio and oil loss in the whole reservoir.

3.6. Recommendations for field development regulation

The regulation of field development is understood as the management of the hydrocarbon extraction process using a set of various technological and technical measures that ensure the best course of the operation process within the framework of the designed development system. The main goals achieved by process regulation are as follows:

- ensuring the dynamics of oil production provided by the design document for the productive formation;

- achievement the design value of the recovery factor at the field;
- improvement of economic indicators by maximizing the use of the drilled wells, reducing the cost of water injection, reducing the production of associated water without compromising oil recovery, etc.

Since the Neocomian and Volga deposits are characterized by extensive sub-gas and water-oil zones, the first years of operation showed that the main problem in the development is a gas breakthrough from the gas cap of the Neocomian sub-layer.

Therefore, to align the inflow profile in the horizontal wells and isolate gas and (or) water breakthroughs, it is recommended to introduce wells with “intelligent” completion, consisting of adjustable section filters that allow the operator to divide the horizontal section into several intervals and, if necessary (gas contamination, flooding) their selective shutdown.

Development of the field control is carried out both on the basis of geological and field data, and using a geological model that allows to adjust the following parameters of the development process:

- operating modes of production wells to avoid uncontrolled gas and water breakthroughs;
- periodic exploitation of wells with gas and water breakthroughs to change the direction of the flows in the reservoir and increase the formation sweep efficiency;
- drilling water and gas injection wells for reservoir pressure maintenance;
- the use of "smart" well equipment to minimize gas and water breakthroughs.

Chapter conclusions

Analyzing the technological part of the Yu. Korchagin field development project, there are several main advantages of the chosen concept of field development, such as:

- Widespread use of fiber optic measurement systems. These systems allow real-time monitoring of the technological regime of the well, to identify discrepancies in production at the early stages, thereby increasing the field development efficiency;

- The use of passive inflow control systems. The use of these systems is one of the most important criteria in the conditions of exploitation of the wells with long reach horizontal sections in the presence of a gas cap and underlying water. These systems also make it possible to increase the efficiency of field development, due to alignment of the inflow profile to a horizontal well, thereby preventing the growth of the gas-oil ratio and water cut of the produced fluid.

Chapter 4. Calculation part

4.1. Analysis of the existing field development concept

Having summed up and analyzed all the information about the development of the Yu. Korchagin field, one can conclude that the field development concept was selected thoroughly, both in technological and technical issues; the offshore structures comply with operating conditions, industrial safety and environmental requirements.

However, the exploitation (the production phase) of the deposit revealed a number of difficulties that could not be analyzed in advance. The most urgent issue requiring special attention was the problem of gas breakthrough from the gas cap into production wells, which significantly reduces the efficiency of the field's production. Such issues become especially acute during the exploitation of marine deposits with a massive gas cap and underlying water. This chapter is dedicated to solving these issues and finding effective technological solutions.

4.2. Analysis of the gas-oil ratio influence on the reserve recovery

During the exploitation of oil and gas condensate deposits, the non-uniformity of the pressure drop in various areas of the reservoir causes the phase contacts to move. The presence of the gas phase in the flow (in particular, the situation that occurs when the reservoir pressure drops at the field) strongly affects the permeability coefficients for oil and water, which ultimately affects the values of the oil and gas recovery coefficients.

The development of the Neocomian deposits of the Yu. Korchagin field is associated with a significant increase in the gas-oil ratio (GOR). When comparing the performance of wells, five of twelve wells revealed discrepancies in the estimated oil production rates with actual data, characterized by a progressive decrease in productivity. The reason for the decline in production was the growth of the gas-oil

ratio, while the actual GOR indicators were more than two times higher than the design values in the considered wells.

Fig. 4.1 presents a graph of the performance dynamics of well No. 1. A 2.5-fold decrease in oil production rates is mainly due to a 4-fold increase of the gas-oil ratio in 3 years of well operation. In particular, during 2013, for this reason, wellhead pressure increased from 8.38 to 9.10 MPa., which indicates gas breakthroughs to the well.

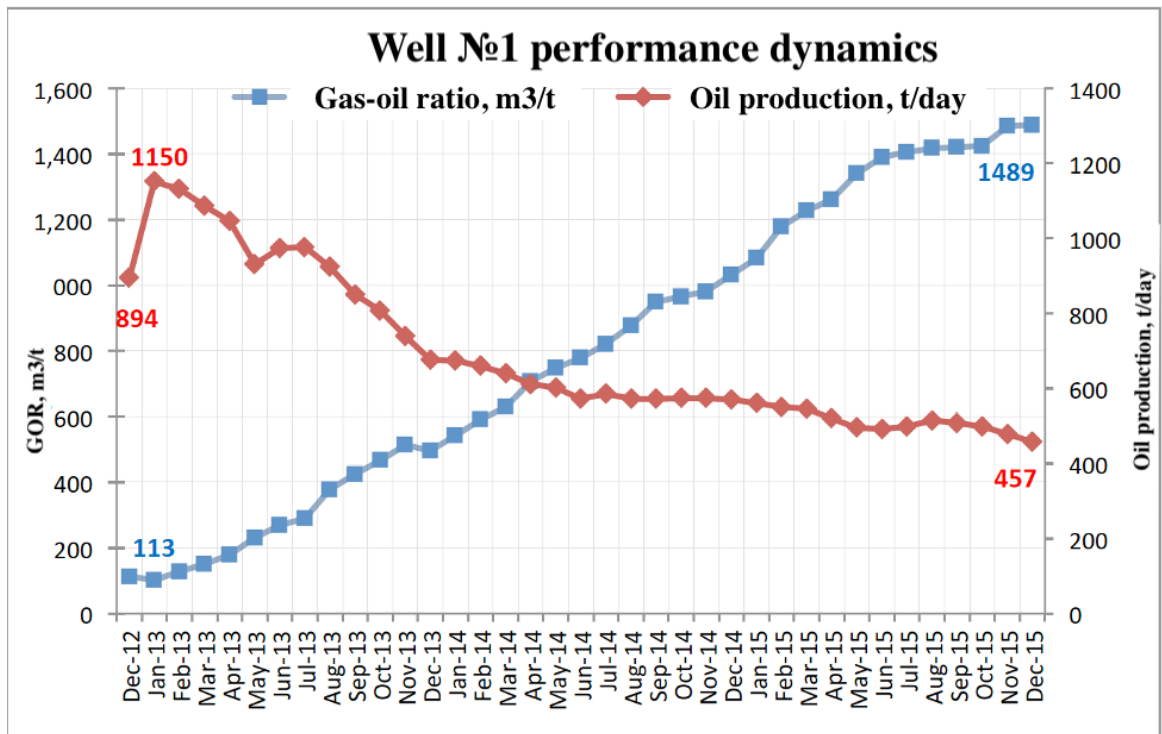


Fig. 4.1 Well №1 performance dynamic

According to [32], during the development of a gas-cap field, when the oil production rate increases (for example, when the bottomhole pressure decreases), the pressure gradient increases, therefore, the surface of the gas-oil contact (GOC) moves to the well. The flow rate is called “critical” when the pressure gradient at the surface of the well increases significantly, and a rapid gas breakthrough occurs, characterized by a vertical inclination of the contact surface.

It is known that the process of oil production from a rim without a gas breakthrough consists of two stages:

1. Vertical gas displacement of oil - a process in which the GOC crest moves to the well, leaving the contacts stable and displacing oil from the volume at a small

distance from the well. With vertical displacement, the viscous forces caused by the pressure gradient influence the velocity of the GOC crest.

2. Gravity drainage is a process in which the GOC crest remains stationary, displacing oil from areas outside the original cone. The displacement of oil and the movement of the contact of the GOC occurs due to the forces of Archimedes.

The contact stability condition is characterized by the values of critical flow rate and critical depression, at which a balance of forces is established, i.e. equality of the hydrodynamic and gravitational gradient at the front:

$$\frac{dp}{dz} = \Delta\rho g.$$

Fig. 4.2 shows a scheme of the oil and gas deposits at the time of formation of the gas cone.

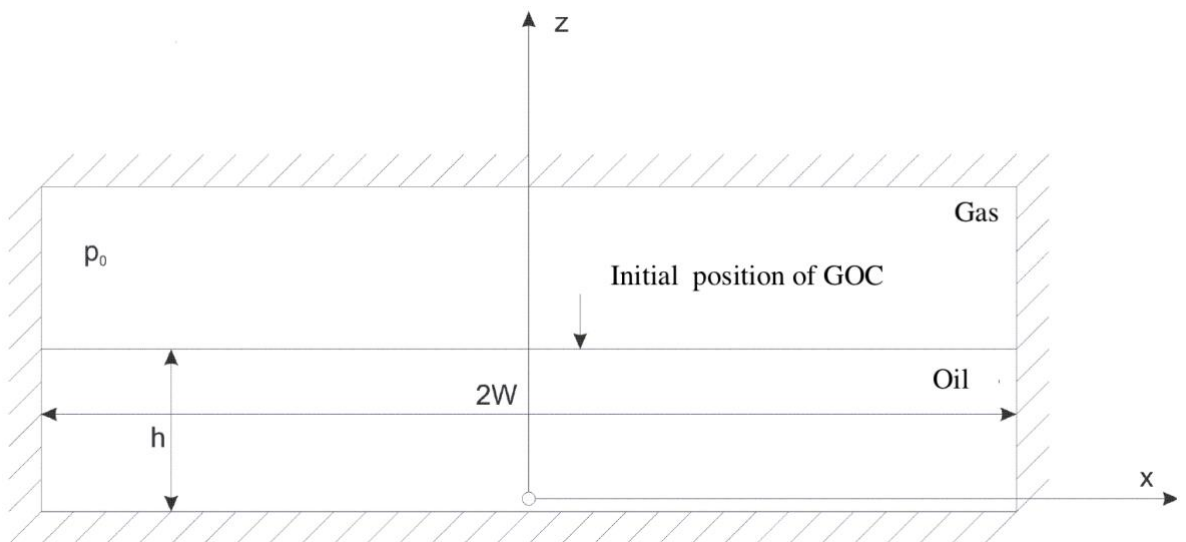


Fig. 4.2 Cross section of horizontal well development element [33]

Using the performance data of well No. 1 as an example for the period from September 2013 to December 2015, the critical flow rate was calculated using the formulas presented by Efros, Giger and Dupui [33].

The formulas for calculating critical flow rates for gravity drainage are presented below:

$$Q_{cr} = \frac{k_R \Delta \rho g}{\mu} \cdot \frac{Lh^2}{W + \sqrt{W^2 + \frac{h^2}{3}}} - \text{Efros formula} \quad (4.1)$$

$$Q_{cr} = \frac{k_R \Delta \rho g}{\mu} \cdot \frac{Lh^2}{W} \left(1 - \frac{1}{6} \left(\frac{h}{W} \right)^2 \right) - \text{Giger formula} \quad (4.2)$$

$$Q_{cr} = \frac{k_R \Delta \rho g}{\mu} \cdot \frac{Lh^2}{W} - \text{Dupuis formula} \quad (4.3)$$

where: k_R – horizontal reservoir permeability, mD;

$\Delta \rho$ – difference between oil and gas density in reservoir conditions, kg/m³;

g – acceleration of gravity, m/s²;

μ – reservoir fluid viscosity, Pa·s;

L – horizontal well length, m;

h – net thickness, m;

W – distance from the center of the well to the top of the contact surface, m.

To solve this problem, the parameters shown in table 4.1 were used. The critical flow rates were calculated by formulas (4.1), (4.2) and (4.3) above. The calculation results are shown in table 4.2.

Table 4.1

The initial data for the Q_{cr} calculation [35]

Parameter, unit	Value
k_R , mD	25
k_z , mD	2.5
$\Delta \rho$, kg/m ³	683
g , m/s ²	9.81
μ , mPa·s	0.65
L , m	2650
h , m	15
W , m	200
ΔS	0.61
m	0.18

where k_z – vertical permeability, m²;

ΔS – difference between initial and residual oil saturation.

Table 4.2

The calculated values of Q_{cr} for well No. 1

Formula	Q_{cr} , m ³ /day/m.
1	0.0107
2	0.0213
3	0.0214

To provide a complete picture of the gas cone's formation, the next stage of the work was to consider the dynamics of critical flow rate by calculating the time dependences of these quantities for the regimes of vertical and gravitational displacement.

From the work [33] it follows that the dependence of the flow rate on time for the vertical displacement mode is calculated as follows:

$$q_{cr(t)} = \frac{2WLk_z\Delta\rho g}{\mu} \cdot \tanh\left(\frac{\pi h}{2W} \sqrt{\frac{k_r}{k_z}} \left(1 - \frac{k_z\Delta\rho g}{\mu m h \Delta S} t\right)\right) \quad (4.4)$$

The dependence of the flow rate on time for the gravity drainage mode is described by the following formula:

$$q_{cr(t)} = \frac{q_{cr}}{\left(1 + \frac{q_{cr}}{V_0} t\right)^2} \quad (4.5)$$

where q_{cr} – critical flow rate;

V_0 – mobile oil reserves at the time of transition to gravity drainage.

The critical flow rate can be founded by the following formula:

$$q_{cr} = \frac{h\Delta\rho gL\sqrt{k_r k_z}}{\mu} q^* \quad (4.6)$$

The given coefficients q^* and W^* are calculated as follows:

$$q^* = e^{0.582} - \sqrt{(\ln W^*)^2 + 0.233 \ln W^* + 0.2} \quad (4.7)$$

$$W^* = \frac{W}{h} \sqrt{\frac{k_z}{k_r}} \quad (4.8)$$

Mobile oil reserves at the time of transition to gravity drainage are equal to the initial moving reserves minus oil production in the vertical displacement mode and are calculated as follows:

$$V_0 = 2WLhm\Delta S \left(1 - \frac{2W}{\pi h} \sqrt{\frac{k_z}{k_r}} \ln \left(\frac{\cosh \left(\frac{\pi h}{2W} \sqrt{\frac{k_z}{k_r}} \right)}{\cosh \left(\frac{\pi h}{2W} \sqrt{\frac{k_z}{k_r}} \left(1 - \frac{t_{transition}}{t} \right) \right)} \right) \right) \quad (4.9)$$

The transition time from vertical displacement to gravity drainage is calculated from the condition of equality of the flow rates of vertical displacement and the initial flow rate of gravity drainage:

$$t_{transition} = \frac{hm\mu}{k_z\Delta\rho g} \left(1 - \frac{\operatorname{arctanh} \frac{hq^*}{2W} \sqrt{\frac{k_z}{k_r}}}{\frac{\pi h}{2W} \sqrt{\frac{k_z}{k_r}}} \right) \quad (4.10)$$

Thus, the time dependence of the critical flow rate of a horizontal well in the under-gas-cap zone of the oil rim is:

$$q_{cr}(t) = \begin{cases} \frac{2WLk_z\Delta\rho g}{\mu} \cdot \tanh\left(\frac{\pi h}{2W}\sqrt{\frac{k_r}{k_z}}\left(1 - \frac{k_z\Delta\rho g}{\mu mh\Delta S}t\right)\right), & t \leq t_{transition} \\ \frac{q_{kp}}{\left(1 + \frac{q_{kp}}{V_0}(t - t_{transition})\right)^2}, & t \geq t_{transition} \end{cases} \quad (4.11)$$

The calculations were carried out with the input data given in table 4.1. The results of the dependence of flow rates and for each regime on time are presented in Fig. 4.3.

As a result of the calculations, it was revealed that the specific oil production rate for a horizontal well should not exceed 0.016 m³/day/m, in general, the production rate should not exceed 42.4 m³/day. The actual production rate of the well exceeds the critical one by about 20 times. Work on flow rates in excess of the calculated values are permissible during the first 15 days of well operation.

The calculations showed that during the development of the field, the oil production rates significantly exceed the calculated, critical production rates, thereby reducing the life of wells with a profitable production rate by several times. In order to increase the efficiency of field development during the subsequent commissioning of new wells, it is necessary to limit the actual oil production, which is, however, not beneficial from the point of view of the project's economy.

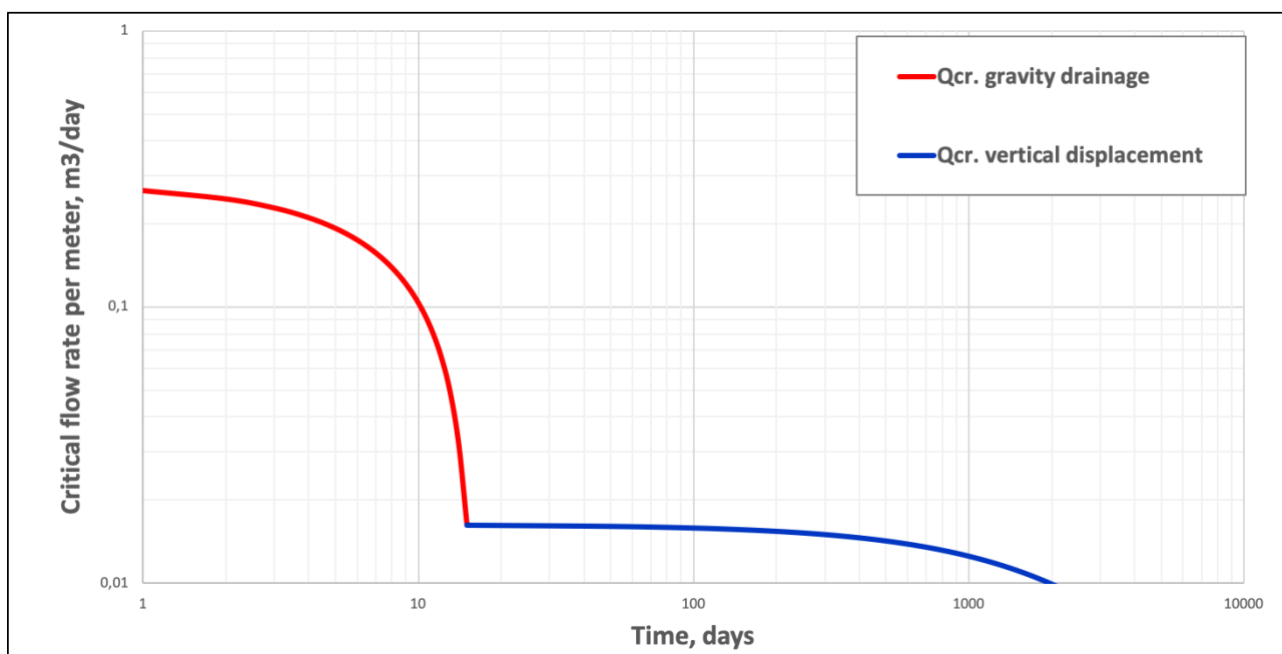


Fig 4.3 Critical flow rate dynamics

As noted above, the critical flow rates obtained during the calculations are so small that they do not ensure the profitability of the project. Therefore, increasing the efficiency of field development was aimed at creating a restriction of gas inflow to the horizontal well, which is ensured by the formation of a "reverse" depression cone, which allows to smooth the contact surface. The creation of a depression cone is achieved through gas withdrawal from the gas-saturated part of the reservoir, by applying a new horizontal sidetrack into the gas reservoir, above the production well.

4.3. Hydrodynamic model

In order to assess the possibility of using barrier wells the hydrodynamic model was built using Schlumberger Petrel software as well as the geological model, which is its foundation. All data used in the model were obtained on the basis of the studies performed, or were evaluated according to the results of experimental data.

Geological model

The geological model consists of 122880 cells and has dimensions of 3200 x 1200 x 80 m. The thickness of the gas cap is 45 m, the oil-saturated zone is 15 m and the water-saturated zone is 20 m. The number of cells in X, Y and Z directions are 32, 48 and 80 respectively. The cell sizes in the X direction are 100 m, Y – 25 m and in the Z direction 1.5, 0.5, and 1.0 m for gas, oil, and water saturated zones, respectively.

The model is homogeneous and has the same permeability values in the XY direction and in the Z direction for all cells (25 and 2.5 mD, respectively). Concerning the porosity, the model also has a uniform distribution, equal to 0.18, with the exception of cells at the model boundary. In these cells, the porosity was artificially inflated to ensure inflow from the outside (the “infinite reservoir” model). The distribution of porosity, horizontal and vertical permeability is shown in Fig. 4.4.

Rock and fluid properties

In the black oil model, the properties of oil and gas, such as gas content, volumetric coefficients and viscosities, are functions of pressure at reservoir

temperature and unchanged phase composition. These properties are determined in laboratory conditions as a result of laboratory experiments on the differential degassing of oil and determination of viscosity.

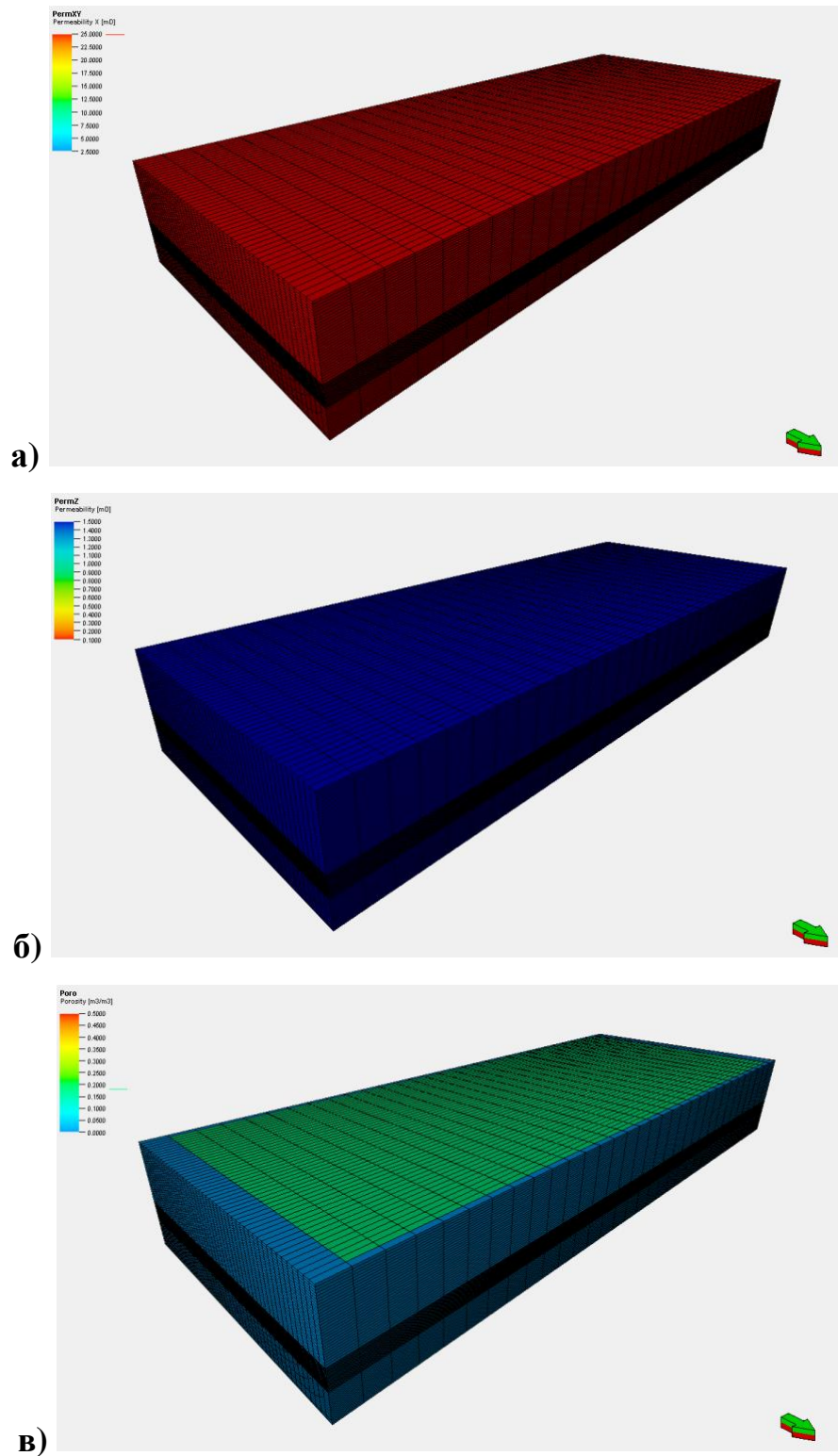
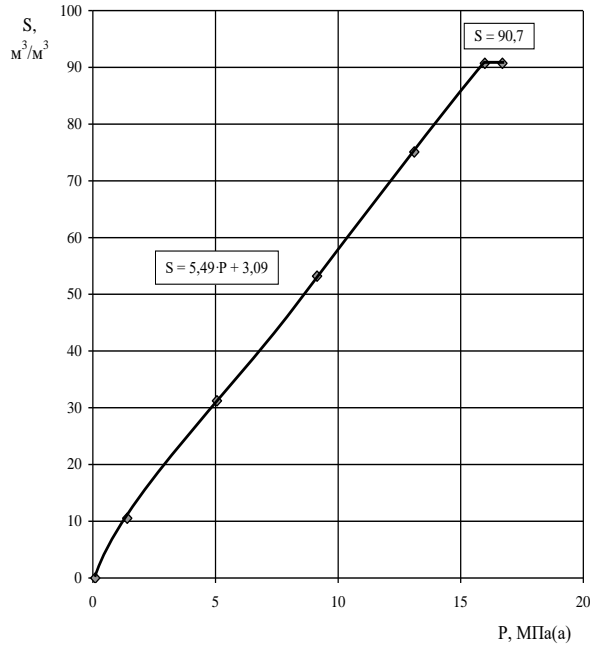


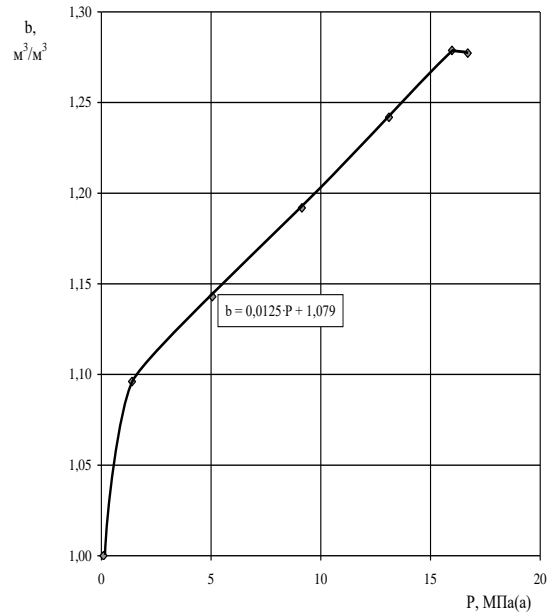
Fig. 4.4 Distribution of a) permeability in the XY direction; b) permeability in the Z direction; c) porosity

To create and convert the model, the data shown in table 4.3 was used, as well as the dependencies for oil and gas, presented in Figs. 4.5 - 4.6.

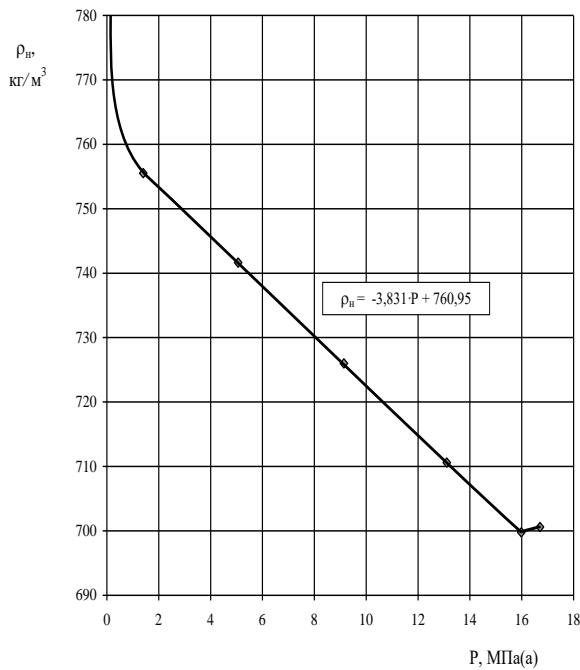
a)



b)



c)



d)

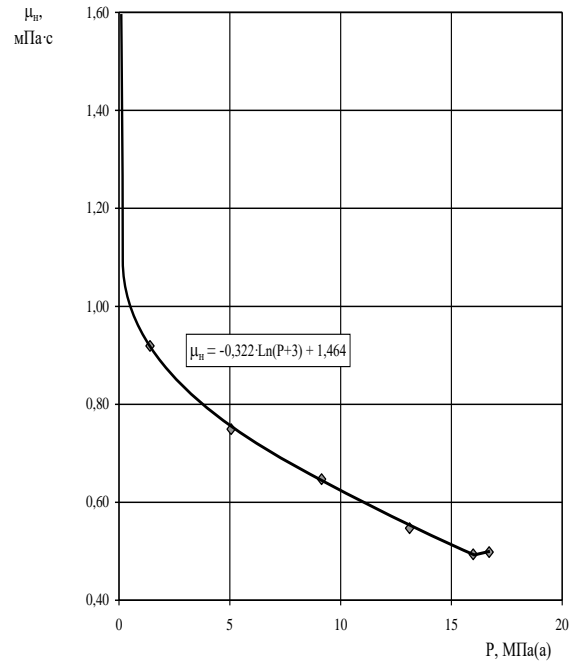


Fig. 4.5 PVT characteristics of oil. Dependence on pressure of: a) gas content, b) volume factor, c) density, d) viscosity

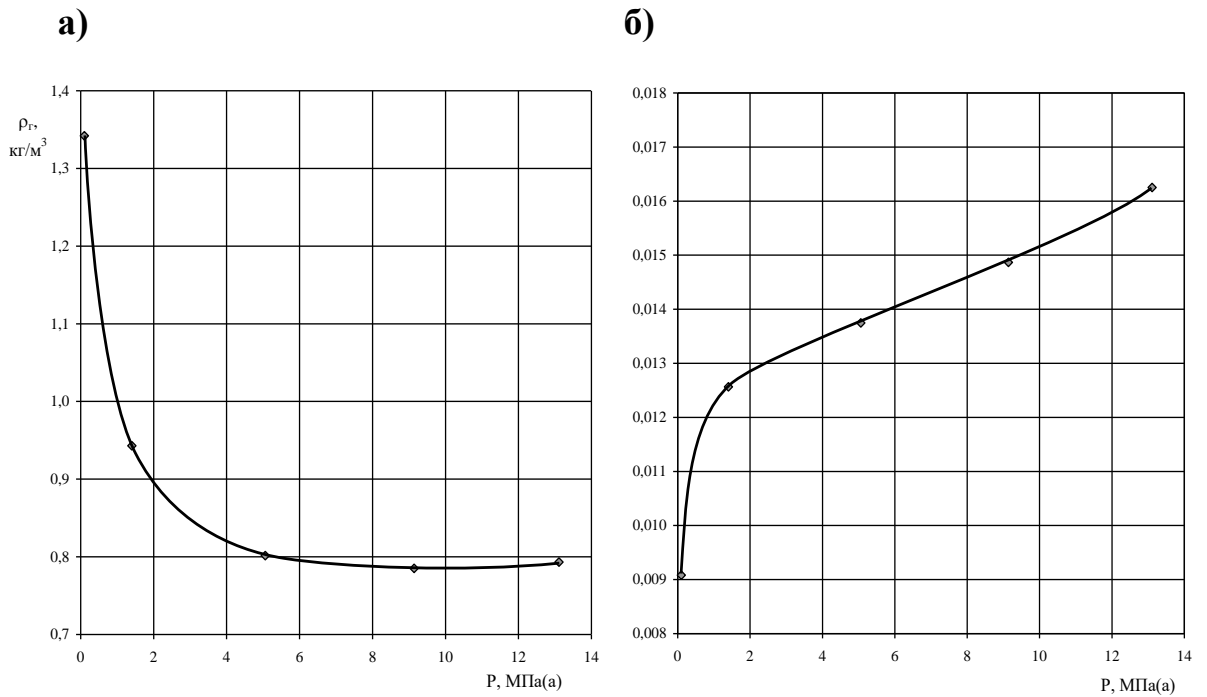


Fig. 4.6 PVT characteristic of gas. Dependence on pressure of: a) density, b) viscosity

Table 4.3

Initial data for PVT model

Parameter, unit	Value
Reservoir temperature, °C	80
Saturation pressure at reservoir temperature, MPa	15.78
Oil density in surface conditions, kg/m^3	813
Density of gas after differential degassing, kg/m^3	0.891
The average value of the oil isothermal compressibility coefficient at reservoir temperature, $1/\text{MPa}$	0.00163
Gas content, m^3/m^3	105.9
Water density in reservoir conditions, kg/m^3	1059

Relative phase permeabilities and capillary pressure

In the case of modeling multi-phase flow, the necessary functions depending on saturation are:

- dependences of relative phase permeabilities for water and oil on water saturation;
- dependence of capillary pressure in the oil-water system on water saturation;
- dependences of relative phase permeabilities for oil and gas on gas saturation;
- dependence of capillary pressure in the oil-gas system on gas saturation [34].

Relative phase permeability is the ratio of rock permeability for a given phase at a given saturation to absolute rock permeability. The relative phase permeability varies from 0 to 1.

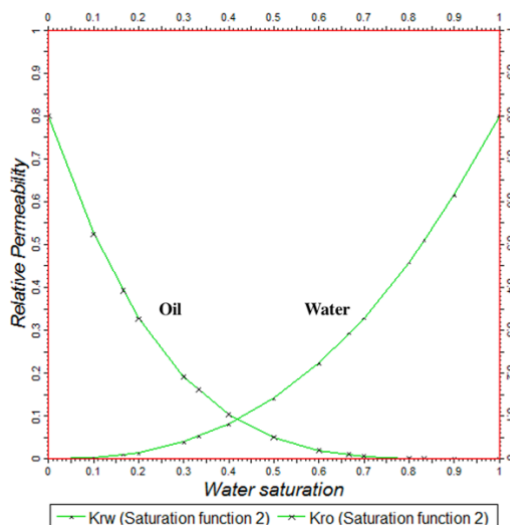
The dependences used for the relative phase permeabilities for the oil-water and oil-gas systems are presented in Fig. 4.7.

Capillary pressure is the pressure difference between two immiscible fluids (phases) that are in equilibrium on both sides of the curved interface. The curvature of the interface occurs due to the preferred wetting of one of these phases of the capillary walls [34].

Capillary pressure curves are used to estimate the distribution of saturation in transition zones at the oil-water, gas-water or gas-oil boundaries in oil and gas fields prior to development.

The capillary pressure curves used for the oil-water and oil-gas systems are shown in Fig. 4.8.

a)



b)

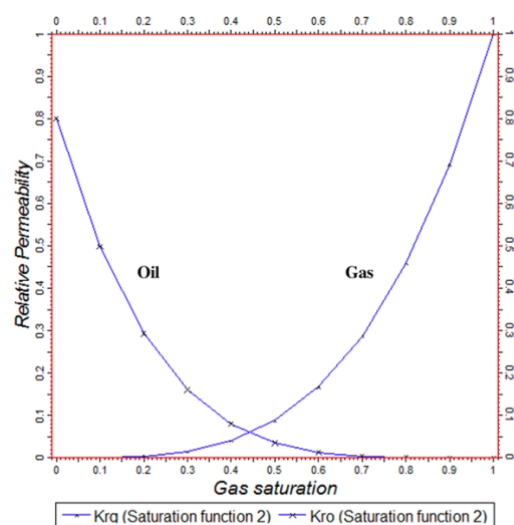


Fig. 4.7 Dependences of relative phase permeabilities for the system a) oil-water, b) oil-gas

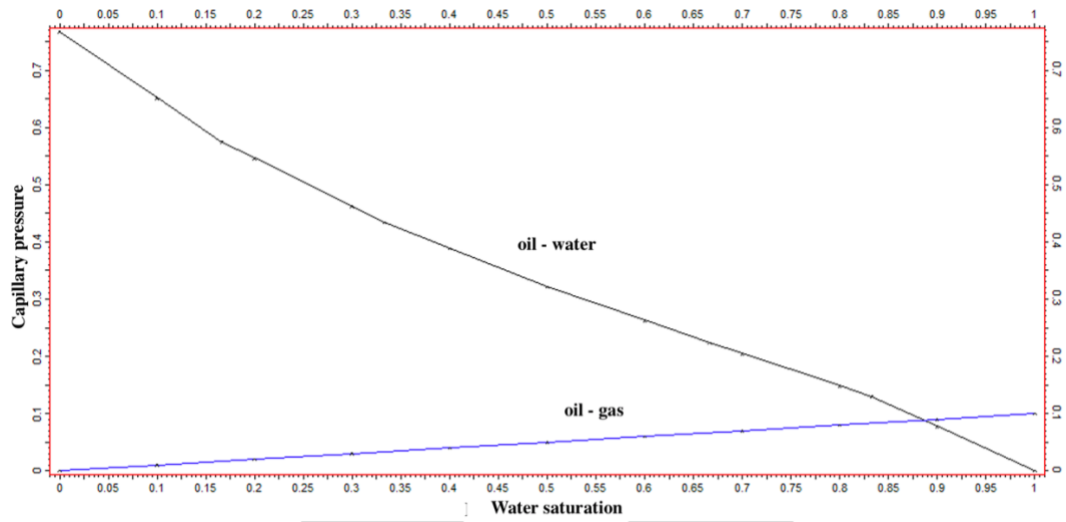
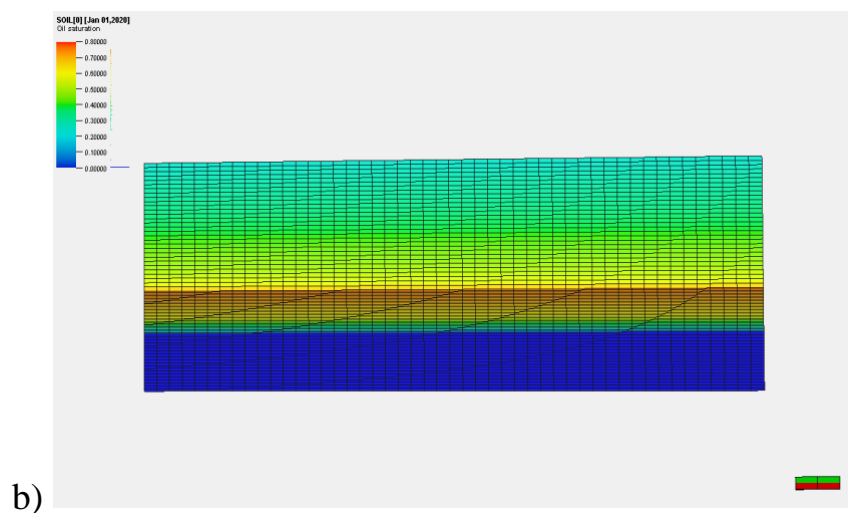
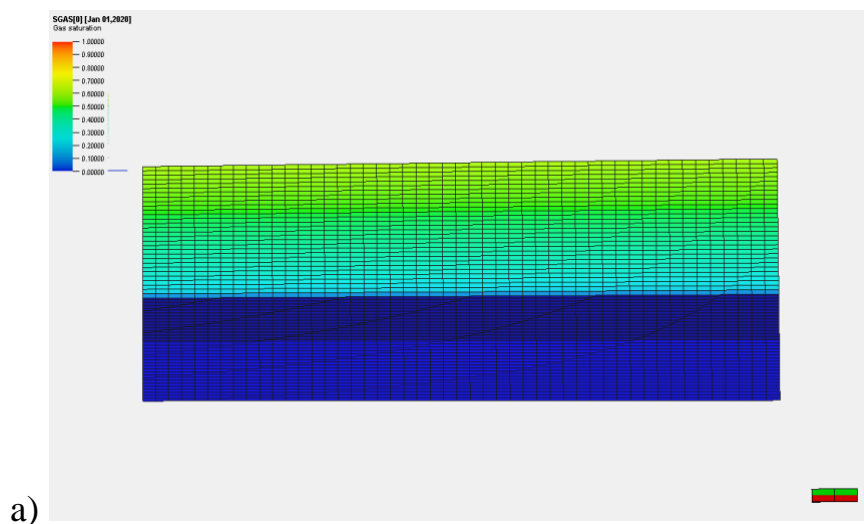


Fig. 4.8 Dependences of capillary pressure for the oil-water and oil-gas systems

Thus, the obtained distributions of gas, oil and water saturation in the model are presented in Fig. 4.9.



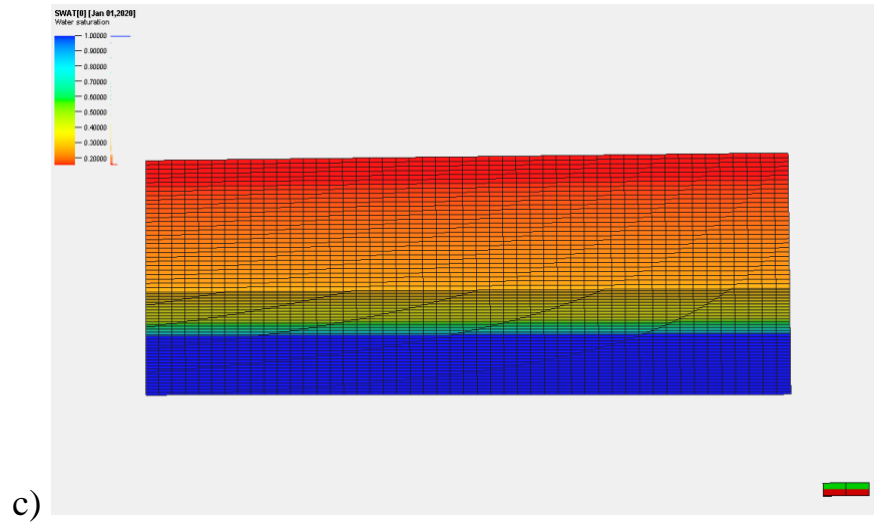


Fig. 4.9 Distribution of a) gas saturation, b) oil saturation, c) water saturation

Model initialization

The parameters specified in table 4.4 were set to initialize the model. The distribution of the initial reservoir pressure is shown in Fig. 4.10.

Table 4.4

Parameters for model initialization

Parameter, unit	Value
Layer cap depth, m	1500
Layer bottom depth, m	1580
Layer cap depth pressure, MPa	16.64
Gas-oil contact, m	1545
Oil-water contact, m	1560

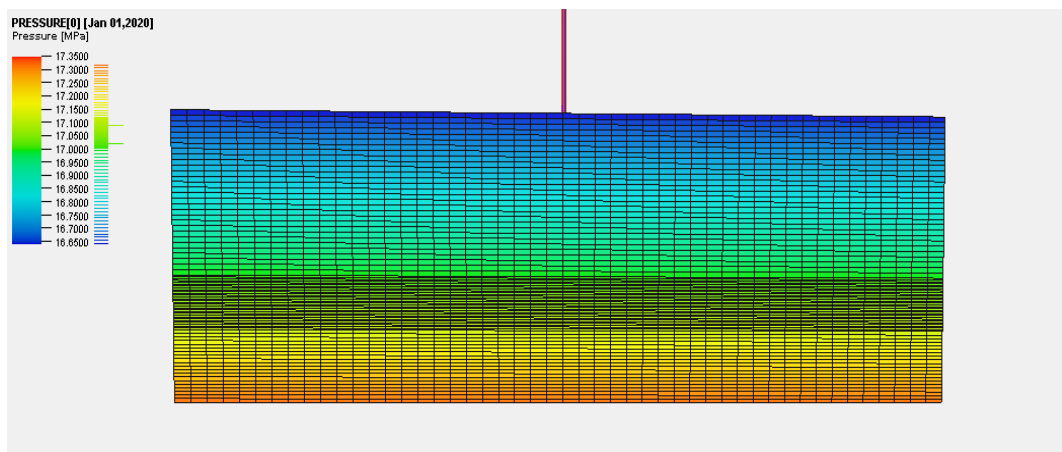


Fig 4.10 Initial reservoir pressure distribution

4.4. Restriction of gas and water inflow to a horizontal oil producing well

Case 1. First of all, in order to evaluate the effectiveness of the proposed measures, it is necessary to calculate the basic case, which assumes the operation of a single well in the oil-saturated zone of the reservoir, which will serve as the basis for comparison with subsequent calculations. For this, one production well must be added to the existing geological model. The well is located along the X axis and is 5 m above the OWC. The well is cased and perforated over the entire length of the horizontal section. Well parameters are presented in table 4.5. The well view on the 3-D model is shown in Fig. 4.11.

Table 4.5

Oil producing well parameters

Parameter, unit	Value
Depth, m	1555
Horizontal section length, m	2600
Diameter, mm	114
Bottomhole pressure, Mpa	16.7

All calculations were performed using the Schlumberger Eclipse software package. The model is calculated for the period 01/01/2013 - 01/01/2020. The results are presented in Fig. 4.12.

As it can be seen on the graph a breakthrough of gas from the gas cap and water from the water-saturated part to the production well started 9 months after the start of exploitation. As a result of this, the oil production rate decreased by almost 2 times in comparison with the initial production rate (from 248 to 123 m³/day), and by the end of the calculation period it decreases by 3.4 times (73 m³/day).

There is also a significant increase in gas production by almost 5 times (from 1828 to 9068 m³/day), and at the end of the calculation period, gas production increases

by almost 15 times in comparison with the initial value. After the breakthrough of water, the water cut of production almost tripled (from 6.5 to 17.5%), and at the end of the calculation period it reached a value of 20.5%.

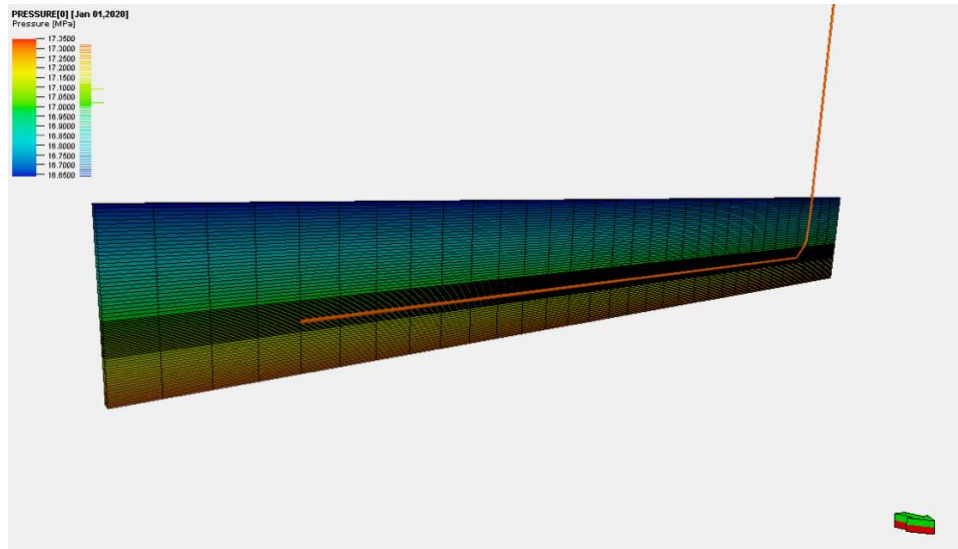


Fig. 4.11 3-D model view for the single well case

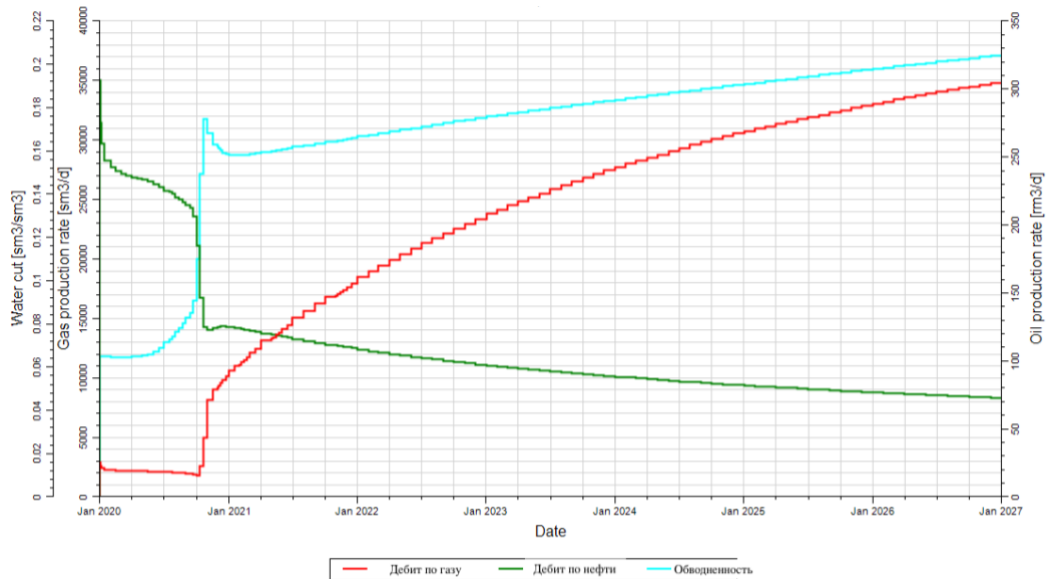


Fig. 4.12 Dynamics of oil, gas flowrates and water cut for the single well case

It should be noted that the values of production rates and water cut obtained as a result of the calculations are used for a qualitative assessment of the process, but not a quantitative, since the constructed model is simplified and does not describe the entire

complexity of the reservoir structure and the processes occurring in it (heterogeneity of the reservoir properties, wells interference).

However, such a simplified model is quite adequate for considering the following cases.

Case 2. The next step is to consider the case with an additional production well located in the gas saturated zone of the reservoir. This well will be located parallel to the main well at a depth of 1535 m. (10 m above the level of GOC). The bottomhole pressure for the oil well was selected so as to ensure the same initial oil production for each case, and the bottomhole pressure of the gas well was selected so as to prevent the formation of a gas cone. Thus, bottomhole pressures for an oil and gas well are 16.20 and 16.15 MPa, respectively. The view of the 3-D model is shown in Fig. 4.13. The results obtained for this case are presented in Fig. 4.14.

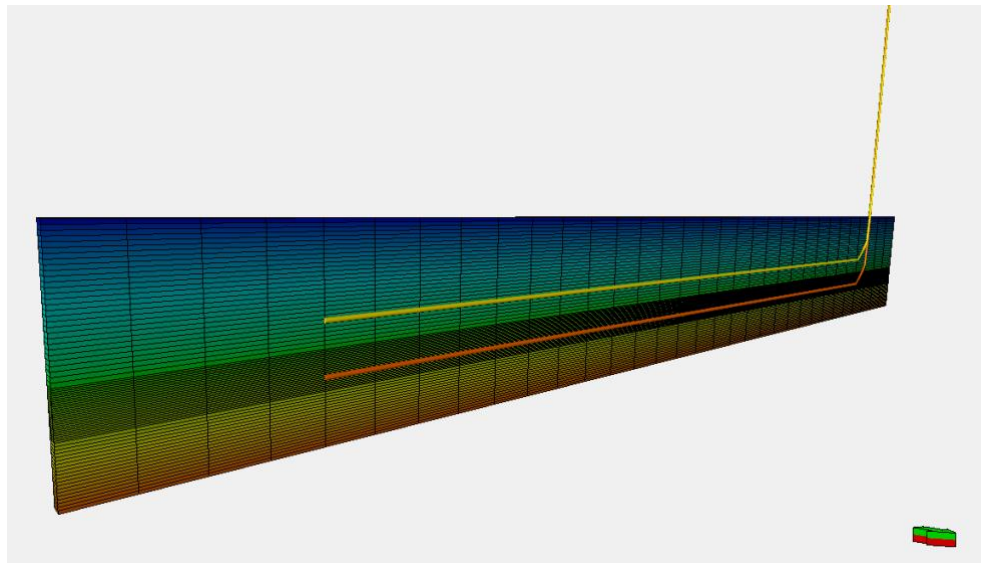


Fig. 4.13 3-D model view for the two wells case

As it can be seen on the graph, the dynamics of oil production is almost identical to the dynamics of gas production. This means that all produced gas is dissolved in oil. Therefore, using gas sampling using an additional well, it was possible to eliminate the breakthrough of gas from the gas cap into the producing well.

However, the problem of water breakthrough from the aquifer remained unresolved. As a result of the formation of a water cone, oil production rate decreases

by more than 2 times during the calculation period (from 250 to 111 m³/day), what significantly affects the amount of cumulative oil production.

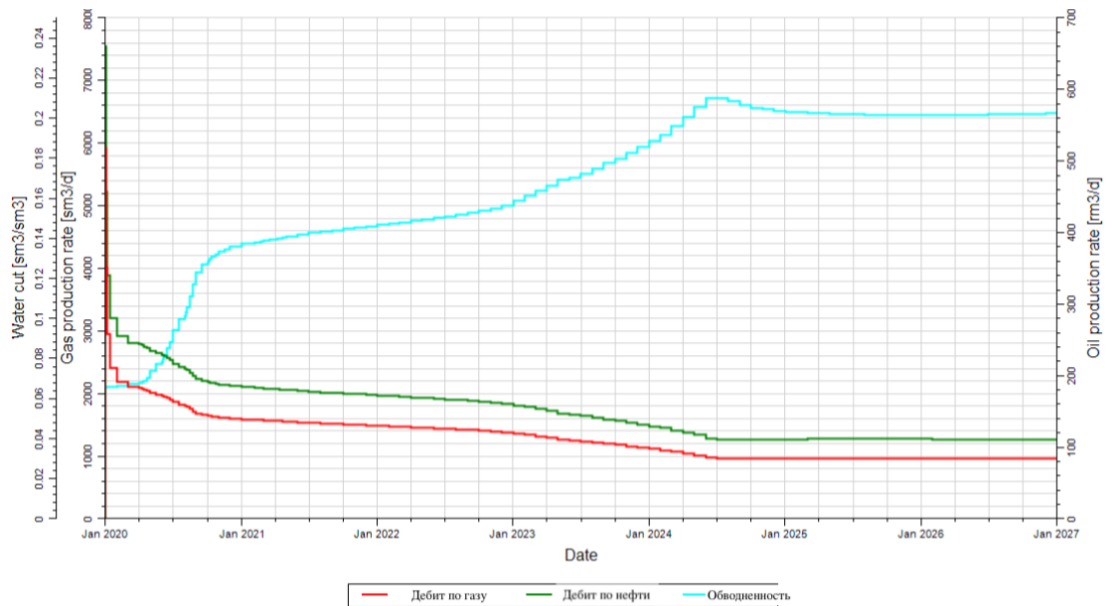


Fig. 4.14 Dynamics of oil, gas flowrates and water cut for the two wells case

Case 3.

The following step was the considering addition of a third well in the water-saturated part of the reservoir, in order to limit the breakthrough of water into the producing well. In this case, the well will also be located parallel to the main well, but at a depth of 1565 m. (5 m below the OWC). The bottomhole pressures of the additional wells, as in the previous case, were calculated in such a way as to prevent breakthroughs of gas and water into the producing well, and the bottomhole pressure of the well in the oil-saturated part of the reservoir was selected in such a way as to ensure compliance with the initial flow rates of previous cases. Thus, bottomhole pressures for oil, gas and water wells are 15.85, 15.35 and 15.75 MPa, respectively. The view of the 3-D model is shown in Fig. 4.15. The results obtained for this case are presented in Fig. 4.16.

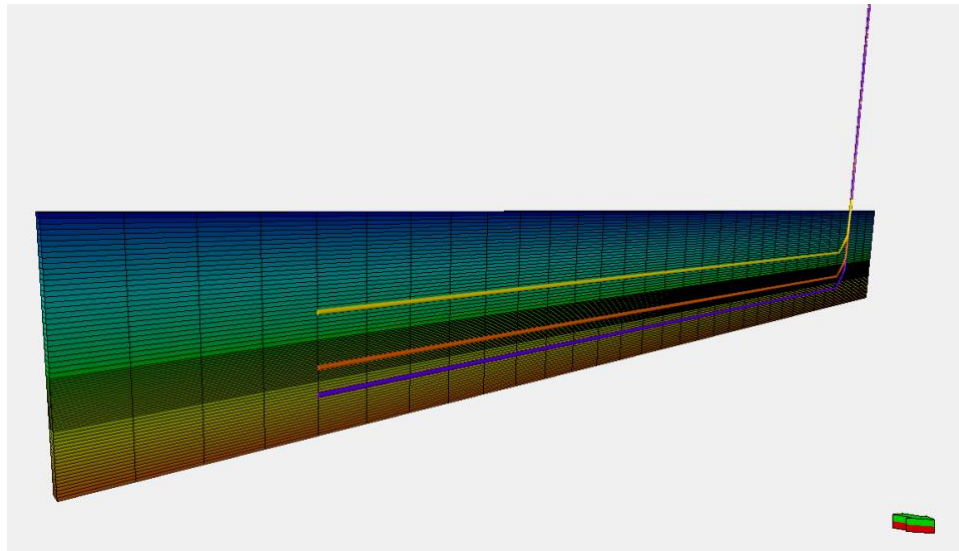


Fig. 4.15 3-D model view for the three wells case

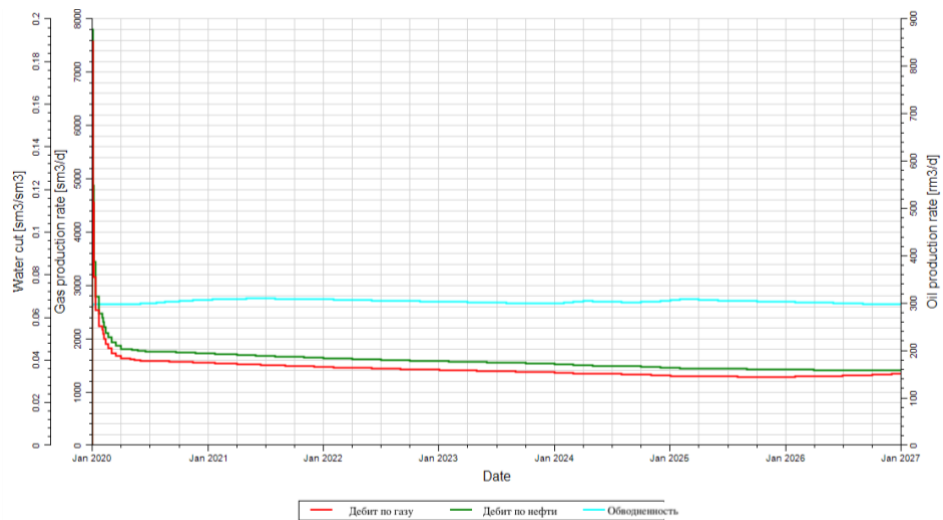


Fig. 4.16 Dynamics of oil, gas flowrates and water cut for the three wells case

As it can be seen on the graph, the dynamics of oil production, as in the previous case, is almost identical to the dynamics of gas production. Consequently, one can conclude that the restriction of gas inflow into the production is still effective. The dynamics of water cut remains almost unchanged. This indicates that due to the introduction of an additional production well in the water-saturated part of the reservoir, it was also possible to limit the breakthrough of water into the main well.

In order to evaluate the effectiveness of the proposed solutions, it is necessary to analyze the cumulative oil production for all three cases. The dynamics of cumulative

production is shown in Fig. 4.17. Table 4.6 shows the numerical values at the end of the calculation period, as well as the change in % in comparison with the base case.

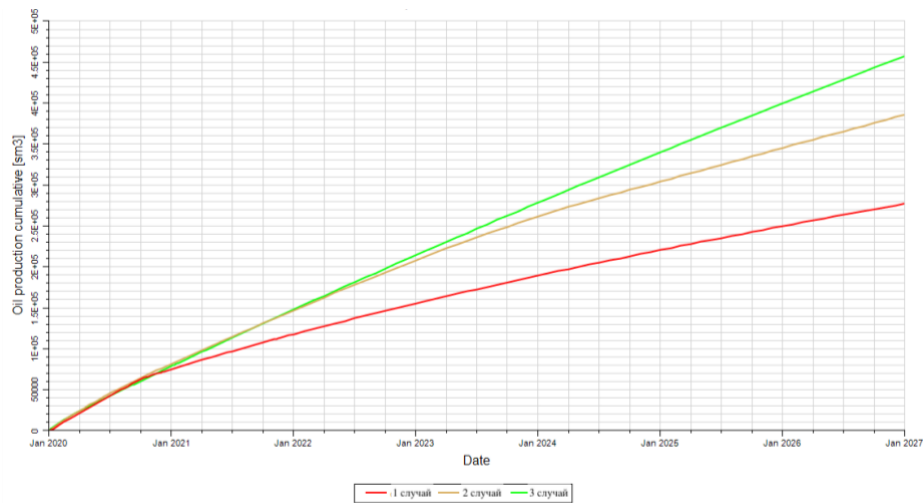


Fig. 4.17 Dynamics of cumulative oil production for three cases

Table 4.6

Comparison of cumulative oil production with a base case

Case	Cumulative oil production, 1000 m ³	Increase in comparison with base case, %
1	277.7	0
2	386.6	39
3	458.6	65

Analyzing the obtained results, one can conclude that the use of "barrier" wells provides an increase in cumulative oil production from 39 to 65% for cases 2 and 3 in comparison with the base case of the field development. In addition, there is a decrease in water cut and gas factor in the main well, thereby one can conclude that the created pressure drawdowns manage to keep the positions of the GOC and OWC in equilibrium. The positive effect of the use of "barrier" wells is to increase the duration of the non-water and non-gas production of oil wells.

However, over time the reserves of the gas cap are depleted and reservoir pressure will decrease significantly. This can lead to a number of negative factors, one

of which is the movement of GOC and OWC upward towards a larger pressure gradient. To avoid this, it is necessary to maintain the pressure in the gas cap by re-injecting the gas.

4.5. Feasibility study

In order to determine the effectiveness of the proposed solution, a feasibility study was carried out according to the indicators of investment costs for well construction and revenue from the sale of produced products.

Investment costs for the implementation of the proposed solution are equal to the costs for the construction of a multilateral well (with two and three branches for the second and third cases, respectively). For calculation, the average specific investment costs for the construction of one meter of the well were used, then, based on these data, the total investment costs for the construction of 6000 m of the wellbore were calculated. The calculation results are presented in table 4.7.

Revenues are calculated based on oil production. Accumulated oil production for well №1 for the considering period amounted to 1 315.8 thousand tons (or 9.5 million barrels). According to the previous calculations, the value of cumulative production will be 1 828.9 thousand tons with barrier wells implementation (or 13.2 million barrels) for the two wells case and 2 171.1 thousand tons (or 15.6 million barrels) for the three wells case. The assumption is made that the volume of oil sold is equal to the volume of oil produced from the well. The calculation was carried out for an oil price equal to \$ 35 per barrel of oil. Revenues are calculated as follows:

$$Revenue = Q \times P \quad (4.5.1)$$

where Q – volume of sold hydrocarbons, barrel;

P – oil price, \$/barrel.

The profit is calculated as the difference between revenue and costs. Profit increase is calculated in comparison with the base case. The calculation results are presented in table 4.8.

Table 4.7

Well construction investment costs [35]

Well type	Construction investment costs, 1000 \$/m	Construction investment costs for 6000 m wellbore, 1000 \$
Horizontal well	5.00	30 000
Sidetracking	2.86	17 160
Multilateral well (2 branches)	7.86	57 160
Multilateral well (3 branches)	10.72	64 320

Table 4.8

Product sales revenue

№	Product Sales Revenue, m\$	Investment costs, m\$	Revenue, m\$	Additional revenue, m\$	Increase in comparison with base case, %
1	332.5	30.00	302.50	0	0
2	462.0	57.16	404.84	102.34	33.8
3	530.4	64.32	466.08	163.58	54.1

At a rough estimate, with the usage of barrier wells, additional profits can range from 550 to 800 million USD for the entire field. Investment costs were calculated as the cost of sidetracking for all producing wells with an average wellbore length of 4700 m. The cumulative oil production was calculated based on actual production, taking

into account an increase of 39 and 65% for the second and third cases, respectively. The calculation results for the field as a whole are shown in table 4.9.

Table 4.9

Revenue from product sales for the entire field

№	Product Sales Revenue, m\$	Investment costs, m\$	Revenue, m\$	Additional revenue, m\$	Increase in comparison with base case, %
1	2 340.8	634.50	1 706.30	0	0
2	3 253.7	997.43	2 256.28	549.98	32.2
3	3 862.3	1 360.37	2 501.95	795.65	46.6

However, it should be understood that in this case, investment costs will not be limited only to the construction of a multilateral well. In this case, it is necessary to build additional water and gas injection wells to re-inject produced gas and water into the reservoir, and it may also be necessary to modernize the offshore platform. Thus, the best option is to use barrier wells only for those wells where the problem of gas breakthrough is manifested to a greater extent.

Also, it should be noted that the above economic assessment allows only indirectly estimate the positive economic effect, for a more accurate feasibility study, a detailed analysis is necessary.

4.6. Technological risks analysis and ways to minimize them

At the first stage, it is necessary to identify risk factors, stages and activities during which the risk arises. Thus, the identification of potential risk areas is a crucial stage of work. If risks are not identified at this stage, they will not be further taken into account in the quantitative analysis.

The application of the proposal for the implementation of two “barrier” production wells in order to increase the volume of cumulative oil production may be

accompanied by a number of technological risks (it should be noted that these are not all possible risks, they are much greater):

- GOC and WOC levels shifting;
- the complexity of the long reach horizontal wells construction and their operation;
- gas and water production higher than acceptable values.
- reservoir pressure drop.

The shifting of both contacts GOC and OWC is associated, first of all, with the beginning of the reserves production. From the beginning of field development, the equilibrium deposit becomes unbalanced. Monitoring of the positions of GOC and OWC allows to increase the period of non-water exploitation of the wells, as well as allows to increase the sweep efficiency and oil recovery factor. The difficulty in constructing long reach horizontal wells and their exploitation lies in a number of factors accompanying well drilling. These include both geological and technological factors (inclinometer accuracy, workforce qualifications, etc.). The potential negative consequences are the loss of the wellbore. The complexity of the operation lies in sealing the joint of the wellbores and ensuring dual string production. Using the completion system according to the international classification (TAML 5) allows to reduce the cost of constructing additional wellbores, the ability to develop three different objects simultaneously and separately, and to provide selective access to all wellbores, as well as allowing the wellbores to be overlapped using a mechanical valve.

The production of gas and water is higher than the acceptable values (the acceptable values in this case are calculated based on the issues of utilization of products and design decisions that are laid at the initial stage of construction). Also, a reservoir pressure drop always accompanies field operations.

After identifying the risks that can lead to negative consequences, one can proceed to develop recommendations for reducing the level of risk. Table 4.10 shows a number of key recommendations to minimize the risks that arise during operation.

Table 4.10

Key recommendations for risks minimizing

Risk	Recommendations
GOC and OWC shifting	<ul style="list-style-type: none"> - bottomhole pressures control and flow rate control (to maintain equilibrium) - control over the positions of the GOC and OWC allows to increase the period of non-water exploitation of the well - allows to increase ORF and sweep efficiency
Long reach horizontal wells construction complexity and their operation;	<ul style="list-style-type: none"> - using the completion system according to the international classification (TAML 5) - shorter wells construction (calculation of the optimal length of the horizontal wellbore)
Gas and water production higher than acceptable values	<ul style="list-style-type: none"> - gas and water injection wells to maintain reservoir pressure - supply of gas and water to the nearest fields
Reservoir pressure drop	<ul style="list-style-type: none"> - gas and water injection wells to maintain reservoir pressure

Conclusion

The conditions of development of the Yu. Korchagin field were analyzed in this work. The causes of the discrepancy between the actual technological indicators and the planned ones are identified, and ways to improve the field development efficiency are proposed.

A preliminary calculation was carried out and the principal possibility of using “barrier” wells in the conditions of an oil deposit with a gas cap and underlying water was shown. The calculation was carried out using a hydrodynamic simulator. The results allow us to conclude that the use of this technology allows to increase technological efficiency by 39 - 65%, and the increase in economic efficiency can reach 33 - 54%.

Obtained results can significantly expand the possibilities of developing such fields in the context of low oil prices and significant depletion of reserves. However, for the actual introduction of the project into work, it is necessary to conduct a more detailed analysis, allowing to take into account all possible risk factors.

References

1. Skobeev, A., Senkov, A., Danilko, A., Volkov, V., & Akhmadiev, R. (2017, October 16). Integrated Approach to Managing of the Offshore Field Development Based on Example of the Yu. Korchagin Field and the V. Filanovsky Field (Russian). Society of Petroleum Engineers. doi:10.2118/187768-RU
2. Amelin N., Leonchik M., Petrov E., Senin B. Caspian without borders // Moscow, Oil and Gas Journal Russia # 5, 2014, p. 38-44.
3. Apollov B. A. The Caspian Sea and its basin / USSR Academy of Sciences. - M.: Publishing House of the Academy of Sciences of the USSR, 1956. - 120 p.
4. Baidin S. S., Kosarev A. N. The Caspian Sea: Hydrology and Hydrochemistry. - M.: Nauka, 1986. -- 261 p.
5. Starodubtsev, Vladimir. (2018). Shoreline changes in the Caspian Sea southern coast.
6. Kasymov, A.G.: "The Caspian Sea", Leningrad (1987)
7. Blagovidov, L. B., & Potapov, V. M. (2006, January 1). Offshore Ice Platforms for the Korchagin Field, North Caspian Sea. International Society of Offshore and Polar Engineers.
8. GRID-Arendal. Mean sea surface temperature on the Caspian Sea. Retrieved from URL: <https://www.grida.no/resources/6115>
9. Shtun, S. Y., Senkov, A. A., Abramenko, O. I., Matsashik, V. V., Mukhametshin, I. R., Prusakov, A. V., & Nukhaev, M. T. (2017, November 1). The Comparison of Inflow Profiling Technologies for ERD Wells Including PLT, Fiber Optics DTS, Stationary Chemical Tracers: A Case Study from the Caspian offshore Yuri Korchagin Field in Russia (Russian). Society of Petroleum Engineers. doi:10.2118/188985-RU
10. Svarovskaya, M., Senkov, A., & Zolotukhin, A. (2014, October 14). Russian Offshore: Gained Experience and Development Perspectives of the Northern

- Block of the Caspian Sea (Russian). Society of Petroleum Engineers.
doi:10.2118/171316-RU
11. Report. "The results of comprehensive hydrodynamic studies and analysis of reservoir fluids of the Yu. Korchagin field", LLC «LUKOIL-Nizhnevolzhskneft», 2012
 12. I. Kibalenko, I. Fyodorov, S. Deliya. Peculiarities in Yuri Korchagin field development // "Neftyanoye Khozyaistvo" No. 3, 2014, M. p. 32–35.
 13. Karulin E. B. and Karulina M. M. Ice model tests of the caisson platform in shallow water, Federal State Unitary Enterprise Krylov State Scientific Center, St. Petersburg, Russia, 2007
 14. Report "Yuri Korchagin Field: the platforms are already at sea", "Caspian Energy Group", 2010
 15. Self-regulatory organization of designers "Western Siberia". Oil Treatment Plant, Deposit them. Yu. Korchagin. Retrieved from URL: <http://www.westsib.org/objects/41>
 16. V.S. Sheinbaum; Ministry of education and science of the Russian Federation, Gubkin Russian State University of Oil and Gas. (NRU), Moscow, 2012-. – 98p.
 17. PrimaMedia. Floating Crane «Bogatyr». Retrieved from URL: <https://primamedia.ru/news/amp/172606/>
 18. United Shipbuilding Corporation. The floating crane "Volgar". Retrieved from: http://www.cmc-heavylift.ru/en/events/detail.php?ELEMENT_ID=43
 19. Offshore Technology. Yuri Korchagin Field, Caspian Sea. Retrieved from: <https://www.offshore-technology.com/projects/yurioffshoreoilfield/attachment/yurioffshoreoilfield3/>
 20. Sea wave. Oil fleet. Retrieved from URL: <http://sea-wave.ru/forum/showthread.php?p=14522&nojs=1>
 21. Report "Caspian project of the Yuri Korchagin field", LLC LUKOIL-Nizhnevolzhskneft, 2011
 22. E. R. Zaderey Analysis and increase of the development efficiency of the Yu. Korchagin field, Krasnoyarsk, Siberian Federal University, 2017.

23. PJSC Lukoil. Press release. Lukoil Completed Installation of the Top Structure of the Block Conductor in the Field Named after Yuri Korchagin. Retrieved from URL: <https://lukoil.ru/PressCenter/Pressreleases/Pressrelease?rid=216801>
24. PJSC Lukoil. Archive. Annual reports and reviews. Retrieved from URL: <https://lukoil.ru/InvestorAndShareholderCenter/ReportsAndPresentations/AnnualReports/ArchiveAnnualReports1999-2009>
25. Confidential document of LLC «LUKOIL-Nizhnevolzhskneft», 2018.
26. Byakov, A., Eliseev, D., Senkov, A., Shafikov, R., Mavrin, A., Lesnoy, A., ... Bulygin, I. (2019, October 22). Completion Technologies Evolution of Yuri Korchagina Wells and Operation Experience of the Intelligent Wells. Society of Petroleum Engineers. doi:10.2118/196923-MS
27. Golenkin, M., Rakitin, M., Shtepin, D., Mityagin, A., Urmantseva, L., Golubtsov, R., ... Cheprasov, A. (2019, October 22). Advanced LWD Technology Application at the Caspian Offshore Oilfields. Society of Petroleum Engineers. doi:10.2118/196959-MS
28. Delia, S. V., Chertenkov, M. V., Zhakovschikov, A. V., Matsashik, V. V., Zhuravlev, O. N., & Shchelushkin, R. V. (2015, October 26). Field Tests of a New Generation of Flow Control Unit Able to Prevent the Gas Breakthrough in Oil Wells. Society of Petroleum Engineers. doi:10.2118/178417-MS
29. Burdin, K., Kichigin, A., Mazitov, R., Lobov, M., Bravkov, P., Stepanov, V., ... Byakov, A. (2015, October 26). Gas Shutoff Treatment in Mega Rich Horizontal Well with Coiled Tubing Inflatable Packer for North Caspian. Society of Petroleum Engineers. doi:10.2118/176688-MS
30. Zhuravlev ON, Nukhaev MT, Shchelushkin RV, Volkov V. Yu. Inflow control devices for completing horizontal wells in the construction of sidetracks in the fields of Western Siberia, WORMHOLES Implementation LLC, Moscow , 2014
31. Confidential document of LLC «LUKOIL-Nizhnevolzhskneft», 2013.
32. Butler R.M. Horizontal wells for oil, gas and bitumen. - M. - Izhevsk, 2010 - 536p.

33. Samolovov D.A. Modeling of oil inflow to horizontal wells in gas-oil zones of oil rims and reservoirs with a gas cap, Tyumen, 2014 -95 p.
34. Pyatibratov P.V. Hydrodynamic modeling of oil field development, Gubkin Russian State University of Oil and Gas, Moscow, 2015 -168s.
35. Confidential document of LLC «LUKOIL-Nizhnevolzhskneft», 2015.